Cytokeratin 15 Can Be Used to Identify the Limbal Phenotype in Normal and Diseased Ocular Surfaces

Satoru Yoshida,[1,2] *Shigeto Shimmura,*[1,2] *Tetsuya Kawakita,*[3] *Hideyuki Miyashita,*[2] *Seika Den,*[3] *Jun Shimazaki,*[2,3] *and Kazuo Tsubota*[1,2]

Purpose. To elucidate the expression pattern of K15, K19, K14, and K12 in human and mouse ocular surface epithelium as putative markers of epithelial phenotype.

Methods. Immunohistochemical staining with specific antibodies for K15, K19, K14, and K12 was performed in human donor cornea tissue and normal ICR mouse corneas, with emphasis on localization of immunopositive cells. Immunohistochemistry was performed in a limbus-deficient mouse model as well as in clinical samples of pannus surgically removed from a thermal burn and a patient with Saltzmann's dystrophy. Staining patterns were classified as limited to the most basal layer (K^{bas}), basal and suprabasal layers ($K^{bas\text{-}sup}$), predominantly in suprabasal layers (K^{sup}) and negative staining (K^-).

Results. In human conjunctival epithelium, strong expression of K15 was observed in basal cells, whereas K19 was expressed in both basal and suprabasal layers ($K15^{bas}/K19^{bas\text{-}sup}/K12^-$). Limbal epithelial cells were $K15^{bas\text{-}sup}/K19^{bas\text{-}sup}/K12^{sup}$, whereas epithelial cells in the central cornea were $K15^-/K19^{bas\text{-}sup}/K12^{bas\text{-}sup}$. In contrast, the mouse ocular surface demonstrated a different expression pattern of K15 and K19 than did the human tissue in the conjunctiva ($K15^{bas\text{-}sup}/K19^{bas}/K12^-$) and the limbus ($K15^{bas\text{-}sup}/K19^{bas}/K12^{sup}$). Neither K15 nor K19 was expressed in the central mouse cornea ($K15^-/K19^-/K12^{bas\text{-}sup}$). Similar cytokeratin expression was observed in conjunctivalized corneas in mice and in surgically removed pannus tissue.

Conclusions. Although the expression of K15 and K19 differ in humans and mice, specific staining patterns can be used to characterize the epithelial phenotype in normal and diseased ocular surface. (*Invest Ophthalmol Vis Sci.* 2006;47: 4780–4786) DOI:10.1167/iovs.06-0574

Keratins (cytokeratins and hair keratins) are a family of cytoskeletal component proteins of epithelial cells. Cytokeratins are divided into two subfamilies: type I (acidic) and type II (basic to neutral). Usually, at least one member of the type I family and one member of the type II family are coordinately expressed in each epithelial cell, and together they form intermediate filaments responsible for the structural integrity of epithelial cells.[1,2] Cytokeratins also seem to play a critical role in tissue differentiation, and the different patterns of cytokeratin expression in epithelia is often used as markers of differentiation.[3–5] For example, it is widely known that differentiated human corneal epithelial cells express cytokeratin 3 (K3, type II) and K12 (type I).[6–9] The cornea-specific expression of K12 has also been found in mice.[10–12] In addition to the predominant expression of K3 and K12, other cytokeratins including K14 and K19 are expressed as minor components of the cytoskeleton in basal and/or suprabasal human corneal epithelial cells.[2,6,13–15]

In the skin, K19 has been proposed as a marker for stem cells in the skin hair follicle and also for proliferative keratinocytes in the basal layer.[16,17] In human ocular surface epithelia, K19 is a minor cytoskeletal component of the corneal epithelium, but it is one of the major components in the conjunctival epithelium where K19 expression is reported to be uniform.[2,6,13–15,18,19] Several studies have reported that K19 expression is found in all layers of the limbal epithelium, which becomes patchy progressively toward the center of the cornea and finally disappears in the center.[2,6,15] K14/K5 expression is believed to be a marker for mitotically active, proliferative basal cells of stratified epithelia.[7] Indeed, K14 expression in the basal layer of corneal epithelium has been reported in humans, mice, and rats.[7,11,14,20] K15 is another type I cytokeratin expressed in stratified epithelia, with several histologic studies reporting the basal expression of K15 in the epidermis.[21–23] Kasper et al.[6] detected K15 protein in corneal and conjunctival epithelium by two-dimensional gel electrophoresis[6]; however, the localization of K15 in ocular surface epithelia remains unknown.

In the present study, K15 was expressed by limbal and conjunctival epithelia, but not by corneal epithelium, in both humans and mice. Furthermore, human limbal epithelium uniquely showed $K15^+$ cells in the suprabasal layers, allowing the distinction of the limbus from conjunctiva. The limbal phenotype can further be characterized by multiple staining with K19 and K12. The pattern of K15 expression, together with other known markers such as ABCG2,[24–26] Cx43,[26,27] and vimentin,[6,14,28,29] can be used to identify basal cells of the limbal area in normal and diseased tissue.

Material and Methods

Mouse Corneas

Specific pathogen-free adult ICR mice (n = 10) were purchased from CLEA Japan, Inc., Tokyo, Japan). All animals were handled in full accordance with the ARVO Statement for the Use of Animals in Ophthalmic and Vision Research and institutional guidelines. To produce total limbal deficiency, we denuded the corneal epithelium including the limbal area with an ophthalmic knife. Re-epithelialization of the scraped cornea was monitored by fluorescein staining. In another group of mice, the ocular surface was air dried for 15 minutes at room temperature under topical anesthesia. After 2 to 4 weeks, the mice were killed by cervical dislocation and the eyes were excised and

From the [1]Cornea Center and the [3]Department of Ophthalmology, Tokyo Dental College, Chiba, Japan; and the [2]Department of Ophthalmology, Keio University School of Medicine, Tokyo, Japan.

Supported in part by a grant from the Advanced and Innovational Research Program in Life Sciences from the Ministry of Education, Culture, Sports, Science and Technology (TK), and a Grant-in-Aid for Scientific Research (SS).

Submitted for publication May 27, 2006; revised July 3, 2006; accepted August 30, 2006.

Disclosure: **S. Yoshida**, None; **S. Shimmura**, None; **T. Kawakita**, None; **H. Miyashita**, None; **S. Den**, None; **J. Shimazaki**, None; **K. Tsubota**, None

The publication costs of this article were defrayed in part by page charge payment. This article must therefore be marked "*advertisement*" in accordance with 18 U.S.C. §1734 solely to indicate this fact.

Corresponding author: Shigeto Shimmura, Keio University School of Medicine, 35 Shinanomachi, Shinjuku-ku, Tokyo 160-8582, Japan; shige@sc.itc.keio.ac.jp.

Investigative Ophthalmology & Visual Science, November 2006, Vol. 47, No. 11

TABLE 1. Antibodies Used in the Study

Antigen	Clone Name/Code	Type	Host	Immunogen	Manufacturer
K12	sc-17101 (L-15)	Polyclonal	Goat	Mouse K12	Santa Cruz Biotechnology, Santa Cruz, CA
K15	LHK15	Monoclonal	Mouse	Human K15	Lab Vision, Fremont, CA
K15	PCK-153P	Polyclonal	Chicken	Human K15	CRP, Denver, CO
K19	RCK108	Monoclonal	Mouse	Human K19	Lab Vision Corp.
K19	RB-9021	Polyclonal	Rabbit	Human K19	Lab Vision Corp.
K19	A53-B/A2.26	Monoclonal	Mouse	Human K19	Chemicon International, Inc., Temecula, CA
K14	PRB-155P	Polyclonal	Rabbit	Mouse K14	CRP
K14	LL001*	Monoclonal	Mouse	Human K14	Abcam Inc., Cambridge MA
K14	SPK14.2*	Monoclonal	Mouse	Human K14	Abcam Inc.
K5	XM26*	Monoclonal	Mouse	Human K5	Abcam Inc.
K5	PRB-160P*	Polyclonal	Rabbit	Mouse K5	CRP

* Used in Supplementary Figure S1, http://www.iovs.org/cgi/content/full/47/11/4780/DC1.

embedded in 4% carboxy methyl cellulose (CMC; Finetec Co., Ltd., Tokyo, Japan) for immunohistochemical staining. Normal, untreated mice were used as the control.

Human Cornea Samples

Normal human corneas (n = 9) were obtained from Northwest Lions Eye Bank (Seattle, WA) and used as the normal control for immunohistochemistry. Clinical samples of pannus tissue were obtained during surgery from a thermal burn patient and a patient with Saltzmann's nodular degeneration. Written informed consent was obtained from each patient before surgery. Excised tissue was immediately embedded in OCT compound (Tissue-Tek; Sakura Finetek, Co. Ltd., Tokyo, Japan) and prepared for immunohistochemistry. The study protocols involving patients and donor eyes were in compliance with the Declaration of Helsinki.

Immunohistochemistry

Immunocytochemistry was performed as described previously.[30] In brief, whole mouse eye or segments of human sclerocorneal tissue were embedded in 4% CMC. Fresh frozen sections (5–10 μm thick) were air dried, fixed in 4% paraformaldehyde for 10 minutes, and then incubated in fixative (Morphosave; Ventana Medical Systems, Tucson, AZ) for 15 minutes. Blocking was performed with 10% donkey or goat serum in phosphate-buffered saline (PBS) for 30 minutes. Sections were then incubated with primary antibodies for 1 hour at room temperature. The primary antibodies used in this study are summarized in Table 1. Immunoreactivity of primary antibodies was visualized with secondary antibodies conjugated with FITC, Cy3 (Jackson ImmunoResearch Laboratories, West Grove, PA) and Alexa 488 (Invitrogen Corp., Carlsbad, CA). After they were washed with PBS, the sections were mounted (Permafluor; Beckman Coulter Inc., Miami, FL). Images were observed by a microscope (Axioplan 2; Carl Zeiss Inc., Thornwood, NY) equipped with a digital camera (Axiocam; Carl Zeiss Inc.). PAS staining was performed according to standard procedures.

Staining patterns of keratin were classified as limited to the most basal layer (K^{bas}), basal and suprabasal layers ($K^{bas\text{-}sup}$), predominantly in suprabasal layers (K^{sup}) and negative staining (K^-).

RESULTS

Cytokeratin Expression on the Human Ocular Surface

We first examined the expression pattern of K15, K19, and K12 on the human ocular surface. As shown in Figures 1B and 2A, strong K15 expression was observed in the basal layer of the conjunctiva, while K19 was expressed in both the basal and suprabasal layers (Fig. 2A). Because K12 was negative (Fig. 1B), the conjunctival epithelial phenotype was $K15^{bas}$/$K19^{bas\text{-}sup}$/$K12^-$. Further into the limbus, K12 expression appeared mainly in the suprabasal layers, although weak staining was observed in the basal cells as well (Figs. 1D, 1E). K19 expression was similar to that in the conjunctiva; however, K15 staining was distinct from the conjunctiva, with positive cells found in the suprabasal layers as well (Figs. 2A, 2C). The number of $K15^+$ layers varied in different sections, even in samples from the same donor (Figs. 1D, 2C, 2F). The limbal epithelial phenotype can thus be represented as $K15^{bas\text{-}sup}$/

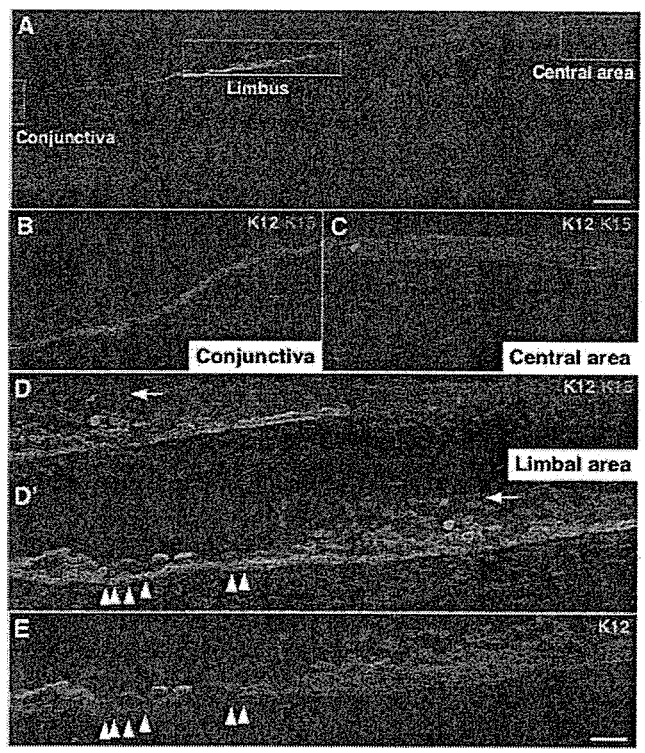

FIGURE 1. Expression of K15 and K12 in human corneal and conjunctival epithelium. (A) An overview of a human ocular surface immunostained with anti-K12 (*green*, FITC) and anti-K15 (*red*, Cy3). *Boxes*: magnified regions shown in conjunctiva (B), central cornea (C), and limbal area (D, D', E). (D, D') Images across the limbus; *white arrow*: same cell in each image. In the conjunctiva, K15 is expressed only in basal cells (B, $K15^{bas}$/$K12^-$). In contrast, $K15^+$ cells were found in the suprabasal layers of the limbus (A, D, D', $K15^{bas\text{-}sup}$/$K12^{sup}$). Isolated $K15^+$ cells were observed in the central area that were also $K12^+$ (C). The expression of K15 was highest in basal cells of the limbal area (D', *arrowheads*). These cells also expressed low levels of K12 (E, *arrowheads*). Scale bar: (A–D') 200 μm; (E) 50 μm.

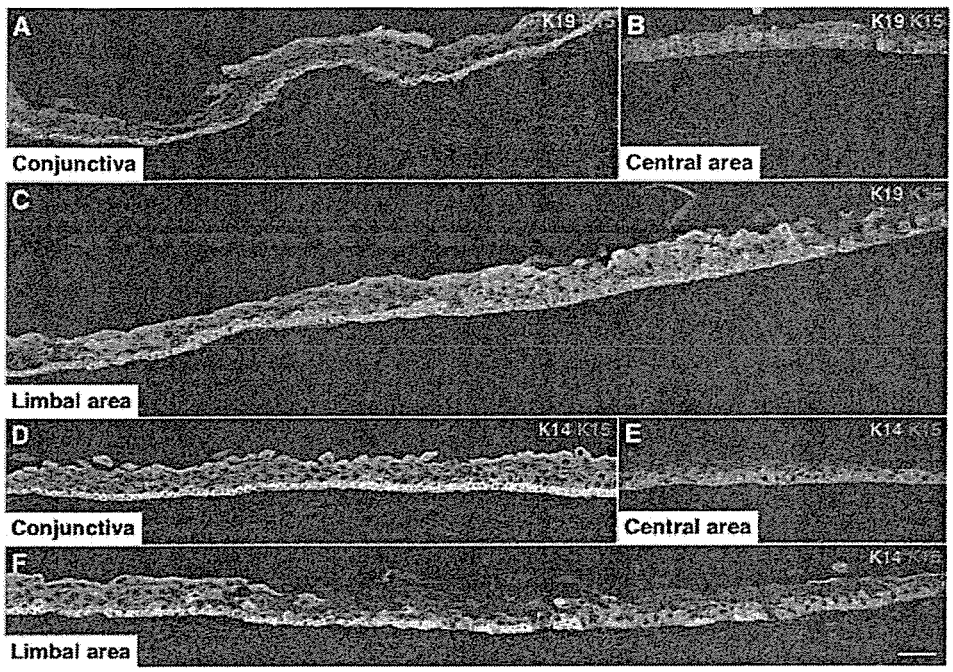

FIGURE 2. Expression pattern of K15, K19, and K14 in human corneal and conjunctival epithelium. Images of serial sections stained with anti-K19 (*green*, FITC) and anti-K15 (*red*, Cy3) antibodies (**A–C**) and with anti-K14 (*green*) and anti-K15 (*red*) antibodies (**D–F**). Conjunctiva (**A**, **D**) and central (**B**, **E**), or limbal area (**C**, **F**) of the cornea. Together with the expression of K15, a strong expression of K19 was observed in the basal and suprabasal layers of the conjunctival ($K15^{bas}/K19^{bas\text{-}sup}$) and limbal ($K15^{bas\text{-}sup}/K19^{bas\text{-}sup}$) epithelia (**A**, **C**, **D**, **F**). Cells weakly positive for K19 were also found in the central area (**B**, $K15^{-}/K19^{bas\text{-}sup}$). K14 was observed in the conjunctiva and in the basal and suprabasal layers of the limbus and central corneal epithelium (**D**, **E**, **F**). Scale bar, 50 μm.

$K19^{bas\text{-}sup}/K12^{sup}$. The central corneal epithelium was uniformly $K12^{+}$ and $K15^{-}$ (Fig. 1C). In addition, as previously reported by Chen et al.,[31] we found various levels of $K19^{+}$ cells in the central corneal epithelium, although the expression level was lower than in the conjunctiva (Fig. 2B). The phenotype of the central cornea was therefore $K15^{-}/K19^{bas\text{-}sup}/K12^{bas\text{-}sup}$.

We further compared the expression of K15 with that of K14, another basal cell marker. Although K14 expression in the corneal epithelium is considered to be restricted to the basal layer,[11,14,20,28,32] we also found K14 staining in the suprabasal layers of corneal and conjunctival epithelium (Figs. 2D–F). Nevertheless, K14 expression was strongest in the $K15^{+}$ basal cells of the limbal and conjunctival epithelium, as well as in $K15^{-}$ corneal basal cells.

Cytokeratin Expression in the Mouse Ocular Surface

We further examined the expression pattern of cytokeratins in mice, and found a contrasting staining pattern in the conjunctiva compared with human tissue. K15 was expressed in all layers of the conjunctival epithelium (Figs. 3A, 3C, 3D), which was similar to the expression of K19 in human conjunctiva. In contrast, K19 was observed only in the most basal layer of the conjunctival epithelium, mirroring that of K15 expression in humans (Figs. 3B, 3C). In other words, K19 and K15 showed a reciprocal pattern in humans and mice ($K15^{bas\text{-}sup}/K19^{bas}/K12^{-}$). As expected, the limbal epithelium was positive for K12 in the suprabasal layer ($K15^{bas\text{-}sup}/K19^{bas}/K12^{sup}$). Cells from the central to midperipheral cornea were predominantly K15 negative (Figs. 3E–G). K19 staining was also negative in the central mouse cornea (Fig. 3F), whereas K12 was positive in the basal and suprabasal layers ($K15^{-}/K19^{-}/K12^{bas\text{-}sup}$).

The expression pattern of K14 in mouse cornea and conjunctiva was similar to human tissue. Strong expression of K14 was observed in the basal and suprabasal cells from the conjunctiva to the limbus (Figs. 3D, 3G). Suprabasal cells in the central area also expressed K14, but the expression level was weak compared with that in the conjunctiva (Fig. 3G).

Cytokeratin Pattern in Identifying Epithelial Phenotype in Pathologic Tissue

Furthermore, we examine the expression pattern of these cytokeratins in conjunctivalized mouse corneas. Debrided corneal epithelium, as well as corneas subjected to severe drying demonstrated the conjunctival phenotype $K19^{bas}/K15^{bas\text{-}sup}/K12^{-}$) in the central cornea (Figs. 4A, 4B, 4D). PAS-positive goblet cells were also observed, confirming the conjunctival phenotype (Fig. 4E).

We finally examined the expression pattern of K15, K19, and K12 in two clinical pannus specimens. In the thermal burn patient, excised tissue clearly showed the conjunctival phenotype $K15^{bas}/K19^{bas\text{-}sup}/K12^{-}$ (Fig. 5). In contrast, pannus tissue from the patient with Saltzmann's nodular degeneration showed patchy staining of all 3 cytokeratins (Fig. 6B). High magnification revealed both the conjunctival phenotype $K15^{bas}/K19^{bas\text{-}sup}/K12^{-}$ and the limbal phenotype $K15^{bas\text{-}sup}/K19^{bas\text{-}sup}/K12^{sup}$ in the same field of view (Figs. 6D–F), suggesting that the epithelium extending into the clear cornea includes basal limbal epithelial cells.

DISCUSSION

Several disorders in humans and mice are caused by deficiencies in cytokeratin genes, suggesting that cytoskeletal proteins have important functions in maintaining cellular integrity.[33] In addition, cytokeratins are often used in the characterization of epithelial phenotype and differentiation and in the diagnosis of carcinomas. K15 is a type I cytokeratin reported in basal keratinocytes of the epidermis[21] and has also been proposed as a marker of stem cells in the hair follicle bulge.[34,35] However, reports on the expression of K15 in the ocular surface are scarce,[6,21] and the expression pattern remains unclear. In this study, we demonstrated the unique expression pattern of K15 in the basal human and mouse corneal and conjunctival epithelium. Different epithelial phenotypes were shown to express unique patterns of K15, K19, and K12 expression (summarized in Table 2).

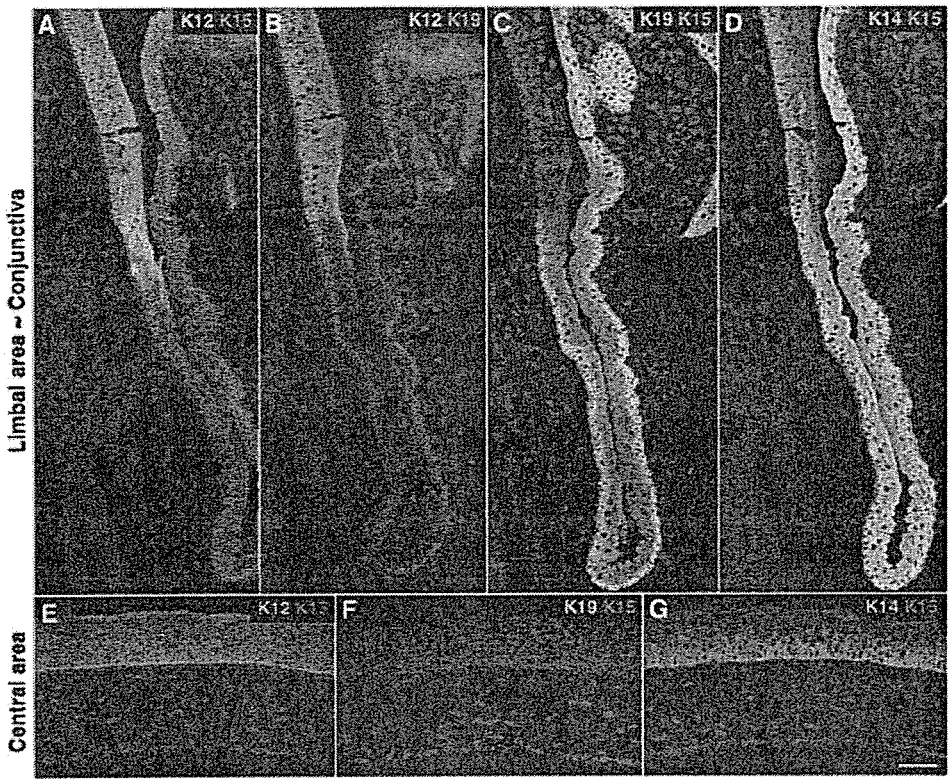

FIGURE 3. Expression of K12, K14, K19, and K15 in mouse corneal and conjunctival epithelium. Images of serial sections stained with anti-K12 (*green*, Alexa-488) and anti-K15 (*red*, Cy3) antibodies (**A**, **E**), anti-K12 (*green*) and anti-K19 (*red*) antibodies (**B**), anti-K19 (*green*) and anti-K15 (*red*) antibodies (**C**, **F**), and anti-K14 (*green*) and anti-K15 (*red*) antibodies (**D**, **G**). (**A**–**D**) Limbal area of mouse cornea and conjunctiva. (**E**–**G**) Central area of the cornea. Characteristic keratin expression patterns were observed in the central cornea ($K15^{-}/K19^{-}/K12^{bas\text{-}sup}$), the limbal area ($K15^{bas\text{-}sup}/K19^{bas}/K12^{sup}$), and the conjunctiva ($K15^{bas\text{-}sup}/K19^{bas}/K12^{-}$). As in human tissue, strong expression of K14 was observed in the basal layer of the cornea and suprabasal cells of the conjunctiva (**D**, **G**). Moderate expression of K14 was observed in suprabasal cells in corneal epithelium (**G**). Scale bar, 50 μm.

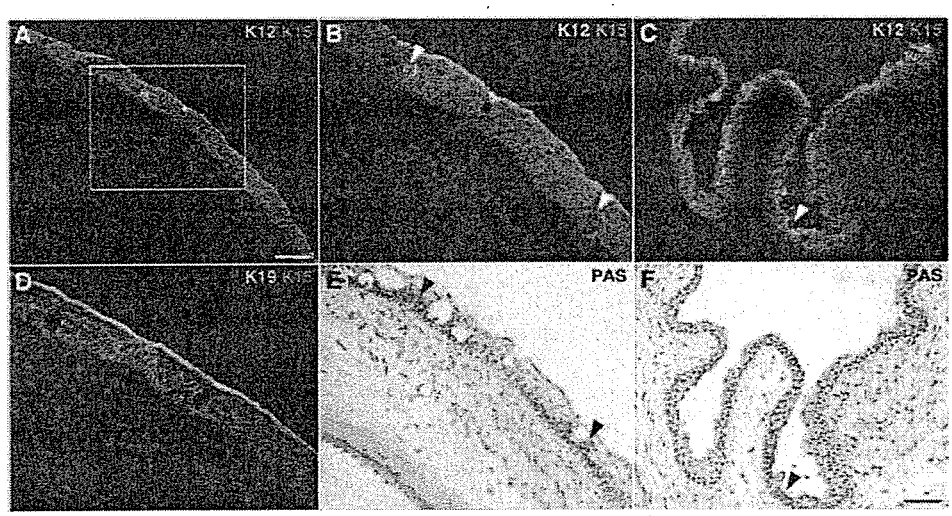

FIGURE 4. Expression of K12, K19, and K15 in conjunctivalized mouse cornea. Sections were stained with anti-K12 (*green*, Alexa-488) and anti-K15 (*red*, Cy3) antibodies (**A**–**C**), anti-K19 (*green*) and anti-K15 (*red*) antibodies (**D**), and PAS (**E**, **F**). (**A**, **B**, **D**, **E**) Central mouse cornea with conjunctivalized epithelium. (**A**) Low-magnification image; *box*: magnified region shown in (**B**). (**C**, **F**) Conjunctival positive control. Conjunctivalization of the cornea is verified by the conjunctival phenotype pattern ($K15^{bas\text{-}sup}/K19^{bas}/K12^{-}$). PAS-positive goblet cells (*black arrowhead*) were also observed (**E**). Background anti-K12 staining was found in goblet cells (*white arrowhead*) in the conjunctiva (**C**) and conjunctivalized cornea epithelium (**B**). Scale bars: (**A**) 100 μm; (**F**) 50 μm.

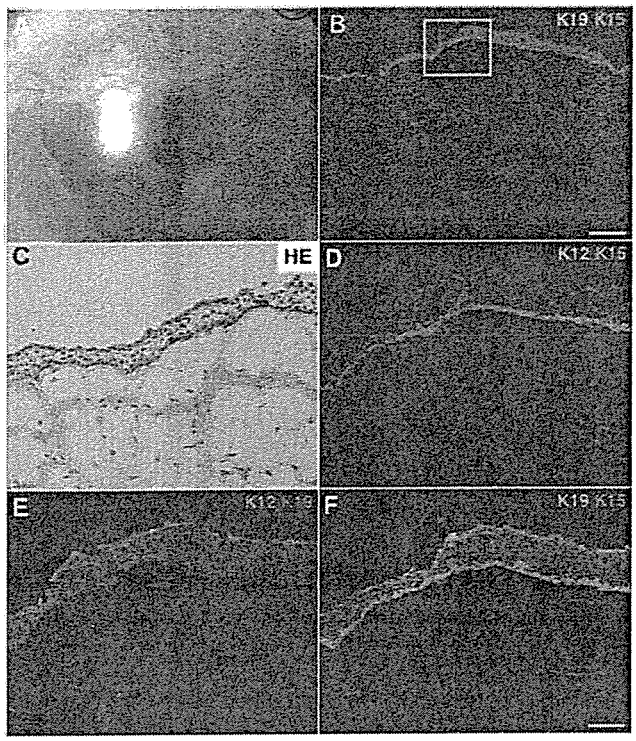

FIGURE 5. Expression of K12, K19, and K15 in a thermal burn patient. (A) Slit micrograph of a vascularized pannus with central corneal phenotype. Hematoxylin-eosin-stained (C) and immunostained (D–F) areas corresponding to the *boxed* region in (B). Serial sections were double stained for K12 (*green*, negative) and K15 (*red*) (D), K12 (*green*, negative) and K19 (*red*) (E), or K19 (*green*) and K15 (*green*) (F). The tissue shows the conjunctiva phenotype $K15^{bas}/K19^{bas\text{-}sup}/K12^{-}$. Scale bars: (B) 200 μm; (F) 50 μm.

It is commonly accepted that in humans, K14 is expressed in the basal layer of the corneal and conjunctival epithelium, and K19 is expressed in basal limbal cells and all layers of the conjunctival epithelium. However, we found K14 in all layers of each stratified epithelia, although the expression level in the suprabasal layers of the corneal epithelium was lower than that in the basal layer. Because the expression of K14 spans the entire length of the ocular surface, it is not useful as a marker to distinguish limbal cells from conjunctival and corneal basal cells. The expression pattern of K19 is also controversial,[19,31] and we found that it is expressed through all layers of the human conjunctival and corneal epithelium, including the limbal area. However, the expression of K19 in the central corneal epithelium showed variation among individuals. Another report by Kasper et al.[6] also showed K19 expressed in all layers of the limbal epithelium.

The difference in the immunohistochemical staining pattern is probably due to variations in technical procedure, which includes the method of tissue processing, the sensitivity of antibodies used, and conditions for visualization. For example, overfixation often leads to loss or reduction of antigen reactivity. Indeed, staining patterns of p63, another gene often used to stain the limbal epithelium, varies greatly in tissue-processing methods.[20] We have confirmed the expression pattern of the cytokeratins demonstrated in this study by using several antibodies for K15, K19, or K14 (Table 1, Supplementary Fig. S1). In addition to K14, we found that K5, a type II partner of K14, is expressed in all layers of the epithelia (Supplementary Fig. S1, online at http://www.iovs.org/cgi/content/full/47/11/4780/DC1), suggesting that the variation in staining mainly depends on the difference in tissue processing rather than the type of antibody used. The condition of the tissue used for immunocytochemistry may also affect keratin expression, because Di Iorio et al.[36] reported that the expression pattern of other stem cell markers depended on the condition of the donor corneas used. However, the elapsed time between death and use of the corneas used in our study was standardized at approximately 5 days (range, 3.5–8.5), and samples were fixed immediately after use for surgery. The variation of cytokeratin expression did not seem to be associated with the variation in elapsed time from death, but rather on the location within a specific sample.

Recently, Kawasaki et al.[37] reported that the K12-positive cells appear to be ectopically residing, self-maintaining corneal epithelial cells in the conjunctival epithelium. We were unable to find such cells in our samples, probably because we did not specifically look for such cell clusters. However, it would be interesting to re-examine such K12-positive clusters in the conjunctiva for K15 expression in the basal and suprabasal layers.

In mice, although expression of K12 and K14 was similar to that in human tissue, strong expression of K15 and K19 was found respectively in the suprabasal and basal layers of the limbal and conjunctival epithelium. The expression pattern of K15 and K19 in mice was exactly the opposite of what was found in human tissue. The data suggest that the functions of these cytokeratins are switched between both species. Both K15 and K19 are type I acidic cytokeratins with undefined type II partners. Because K15 and K19 are not expressed in the

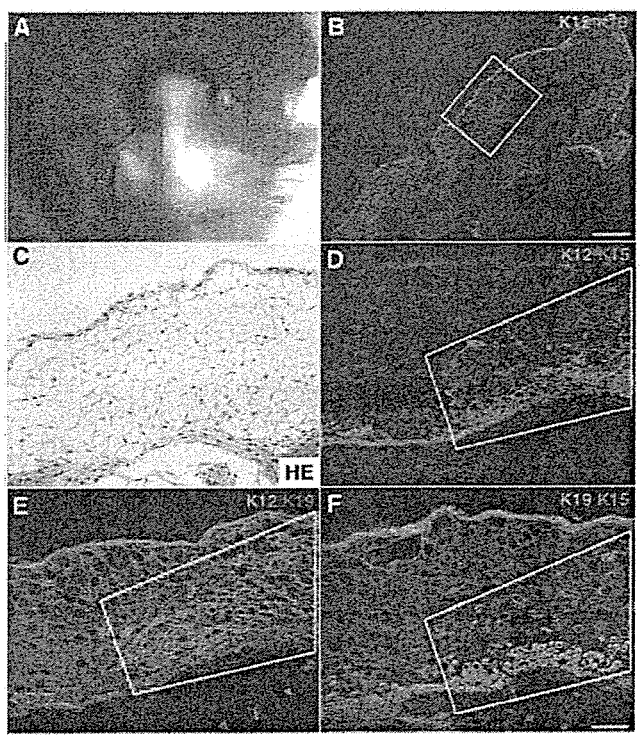

FIGURE 6. Expression of K12, K19, and K15 in a Saltzmann's nodular degeneration patient. (A) Presurgical slit micrograph of the pannus extending from the inferior nasal quadrant of the right eye. Hematoxylin-eosin-stained (C) and immunostained (D–F) images of the area corresponding to the *boxed* region in (B). Serial sections were double stained for K12 (*green*, negative) and K15 (*red*) (D), K12 (*green*, negative) and K19 (*red*) (E), or K19 (*green*) and K15 (*green*) (F). Both the conjunctival phenotype $K15^{bas}/K19^{bas\text{-}sup}/K12^{-}$ and limbal phenotype $K15^{bas\text{-}sup}/K19^{bas\text{-}sup}/K12^{sup}$ (D–F, *boxes*) were observed in this tissue. Scale bar, 50 μm.

TABLE 2. Summary of K12, K14, K15, and K19 Expression in Human and Mouse Ocular Surface Epithelium

	Conjunctiva		Limbal Area		Central Area	
	Basal	Suprabasal	Basal	Suprabasal	Basal	Suprabasal
Human	$K15^{bas}/K19^{bas\text{-}sup}/K12^{-}$		$K15^{bas\text{-}sup}/K19^{bas\text{-}sup}/K12$		$K15^{-}/K19^{bas\text{-}sup}/K12^{bas\text{-}sup}$	
K12	−	−	+/−	+/−	++	++
K15	+++	−	+++*	++/+/−*	−†	−†
K19	+++	++	+++	++	+	+
K14	+++	++	+++	++	+++	
Mouse	$K15^{bas\text{-}sup}/K19^{bas}/K12^{-}$		$K15^{bas\text{-}sup}/K19^{bas}/K12^{sup}$		$K15^{-}/K19^{-}/K12^{bas\text{-}sup}$	
K12	−	−	+/−	+/−	++	++
K15	+	++	+	++	−	−
K19	++	−‡	++	−‡	−	−
K14	+++	++	+++	++	+++	+

* The number of K15-positive cells vary in different sections.
† Occasional positive cell.
‡ Background staining.

central cornea ($K15^{-}/K19^{-}/K12^{bas\text{-}sup}$), both can be used to demonstrate conjunctivalization in mice. The possibility that antibodies for K15 and K19 cross-react respectively with K19 and K15 in mice cannot be completely ruled out. However, this is highly unlikely when the amino acid sequences of the cytokeratins are compared in both species.

Although cytokeratin expression alone is not sufficient to identify stem cells or transient amplifying (TA) cells, the expression profile of several key cytokeratins can be used to characterize epithelial phenotype in normal and diseased tissue. We have also identified K15 as a key cytokeratin that, unlike K14, is not expressed in differentiated corneal epithelium, and can also be used to differentiate limbal phenotype from the conjunctiva. Indeed, the human limbal phenotype $K15^{bas\text{-}sup}/K19^{bas\text{-}sup}/K12^{sup}$ was found in surgically removed tissue that was clinically diagnosed as invading conjunctival epithelium. Therefore, this staining combination may be used to identify residual limbal structures in limbal deficient eyes.

Acknowledgments

The authors thank Kimie Kato for technical assistance.

References

1. Irvine AD, McLean WH. Human keratin diseases: the increasing spectrum of disease and subtlety of the phenotype-genotype correlation. *Br J Dermatol.* 1999;140:815–828.
2. Pitz S, Moll R. Intermediate-filament expression in ocular tissue. *Prog Retin Eye Res.* 2002;21:241–262.
3. Fuchs E. Keratins as biochemical markers of epithelial differentiation. *Trends Genet.* 1988;4:277–281.
4. Sun TT, Eichner R, Nelson WG, et al. Keratin classes: molecular markers for different types of epithelial differentiation. *J Invest Dermatol.* 1983;81:109S–115S.
5. Tseng SC, Jarvinen MJ, Nelson WG, et al. Correlation of specific keratins with different types of epithelial differentiation: monoclonal antibody studies. *Cell.* 1982;30:361–372.
6. Kasper M, Moll R, Stosiek P, Karsten U. Patterns of cytokeratin and vimentin expression in the human eye. *Histochemistry.* 1988;89:369–377.
7. Moll R, Franke WW, Schiller DL, Geiger B, Krepler R. The catalog of human cytokeratins: patterns of expression in normal epithelia, tumors and cultured cells. *Cell.* 1982;31:11–24.
8. Sun TT, Tseng SC, Huang AJ, et al. Monoclonal antibody studies of mammalian epithelial keratins: a review. *Ann NY Acad Sci.* 1985;455:307–329.
9. Tanifuji-Terai N, Terai K, Hayashi Y, Chikama T, Kao WW. Expression of keratin 12 and maturation of corneal epithelium during development and postnatal growth. *Invest Ophthalmol Vis Sci.* 2006;47:545–551.
10. Kao WW, Liu CY, Converse RL, et al. Keratin 12-deficient mice have fragile corneal epithelia. *Invest Ophthalmol Vis Sci.* 1996;37:2572–2584.
11. Kurpakus MA, Maniaci MT, Esco M. Expression of keratins K12, K4 and K14 during development of ocular surface epithelium. *Curr Eye Res.* 1994;13:805–814.
12. Liu CY, Zhu G, Westerhausen-Larson A, et al. Cornea-specific expression of K12 keratin during mouse development. *Curr Eye Res.* 1993;12:963–974.
13. Elder MJ, Hiscott P, Dart JK. Intermediate filament expression by normal and diseased human corneal epithelium. *Hum Pathol.* 1997;28:1348–1354.
14. Kasper M, Stosiek P, Lane B. Cytokeratin and vimentin heterogeneity in human cornea. *Acta Histochem.* 1992;93:371–381.
15. Kivela T, Uusitalo M. Structure, development and function of cytoskeletal elements in non-neuronal cells of the human eye. *Prog Retin Eye Res.* 1998;17:385–428.
16. Lyle S, Christofidou-Solomidou M, Liu Y, et al. The C8/144B monoclonal antibody recognizes cytokeratin 15 and defines the location of human hair follicle stem cells. *J Cell Sci.* 1998;111:3179–3188.
17. Michel M, Torok N, Godbout MJ, et al. Keratin 19 as a biochemical marker of skin stem cells in vivo and in vitro: keratin 19 expressing cells are differentially localized in function of anatomic sites, and their number varies with donor age and culture stage. *J Cell Sci.* 9:1017-.
18. Espana EM, Di Pascuale MA, He H, et al. Characterization of corneal pannus removed from patients with total limbal stem cell deficiency. *Invest Ophthalmol Vis Sci.* 2004;45:2961–2966.
19. Schlotzer-Schrehardt U, Kruse FE. Identification and characterization of limbal stem cells. *Exp Eye Res.* 2005;81:247–264.
20. Hsueh YJ, Wang DY, Cheng CC, Chen JK. Age-related expressions of p63 and other keratinocyte stem cell markers in rat cornea. *J Biomed Sci.* 2004;11:641–651.
21. Lloyd C, Yu QC, Cheng J, et al. The basal keratin network of stratified squamous epithelia: defining K15 function in the absence of K14. *J Cell Biol.* 1995;129:1329–1344.
22. Porter RM, Lunny DP, Ogden PH, et al. K15 expression implies lateral differentiation within stratified epithelial basal cells. *Lab Invest.* 2000;80:1701–1710.
23. Waseem A, Dogan B, Tidman N, et al. Keratin 15 expression in stratified epithelia: downregulation in activated keratinocytes. *J Invest Dermatol.* 1999;112:362–369.
24. Budak MT, Alpdogan OS, Zhou M, et al. Ocular surface epithelia contain ABCG2-dependent side population cells exhibiting features associated with stem cells. *J Cell Sci.* 2005;118:1715–1724.
25. Watanabe K, Nishida K, Yamato M, et al. Human limbal epithelium contains side population cells expressing the ATP-binding cassette transporter ABCG2. *FEBS Lett.* 2004;565:6–10.

26. Wolosin JM, Budak MT, Akinci MA. Ocular surface epithelial and stem cell development. *Int J Dev Biol.* 2004;48:981–991.
27. Matic M, Petrov IN, Chen S, et al. Stem cells of the corneal epithelium lack connexins and metabolite transfer capacity. *Differentiation.* 1997;61:251–260.
28. Kasper M. Patterns of cytokeratins and vimentin in guinea pig and mouse eye tissue: evidence for regional variations in intermediate filament expression in limbal epithelium. *Acta Histochem.* 1992; 93:319–332.
29. Lauweryns B, van den Oord JJ, Missotten L. The transitional zone between limbus and peripheral cornea: an immunohistochemical study. *Invest Ophthalmol Vis Sci.* 1993;34:1991–999.
30. Yoshida S, Shimmura S, Shimazaki J, Shinozaki N, Tsubota K. Serum-free spheroid culture of mouse corneal keratocytes. *Invest Ophthalmol Vis Sci.* 2005;46:1653–658.
31. Chen Z, de Paiva CS, Luo L, et al. Characterization of putative stem cell phenotype in human limbal epithelia. *Stem Cells.* 2004;22: 355–366.
32. Kasper M. Heterogeneity in the immunolocalization of cytokeratin specific monoclonal antibodies in the rat eye: evaluation of unusual epithelial tissue entities. *Histochemistry.* 1991;95:613–620.
33. Porter RM, Lane EB. Phenotypes, genotypes and their contribution to understanding keratin function. *Trends Genet.* 2003;19:278–285.
34. Liu Y, Lyle S, Yang Z, Cotsarelis G. Keratin 15 promoter targets putative epithelial stem cells in the hair follicle bulge. *J Invest Dermatol.* 2003;121:963–968.
35. Morris RJ, Liu Y, Marles L, et al. Capturing and profiling adult hair follicle stem cells. *Nat Biotechnol.* 2004;22:411–.
36. Di Iorio E, Barbaro V, Ruzza A, et al. Isoforms of DeltaNp63 and the migration of ocular limbal cells in human corneal regeneration. *Proc Natl Acad Sci USA.* 2005;102:9523–9528.
37. Kawasaki S, Tanioka H, Yamasaki K, et al. Clusters of corneal epithelial cells reside ectopically in human conjunctival epithelium. *Invest Ophthalmol Vis Sci.* 2006;47:1359–1367.

STEM CELLS
TISSUE-SPECIFIC STEM CELLS

Isolation of Multipotent Neural Crest-Derived Stem Cells from the Adult Mouse Cornea

SATORU YOSHIDA,[a,b] SHIGETO SHIMMURA,[a,b] NARIHITO NAGOSHI,[c] KEIICHI FUKUDA,[d] YUMI MATSUZAKI,[c] HIDEYUKI OKANO,[c] KAZUO TSUBOTA[a,b]

[a]Cornea Center, Tokyo Dental College, Ichikawa, Chiba, Japan; [b]Department of Ophthalmology, Keio University School of Medicine, Shinjuku-ku, Tokyo, Japan; [c]Department of Physiology, Keio University School of Medicine, Shinjuku-ku, Tokyo, Japan; [d]Department of Regenerative Medicine and Advanced Cardiac Therapeutics, Keio University School of Medicine, Shinjuku-ku, Tokyo, Japan

Key Words. Corneal stroma • Keratocyte • Stem cells • Bone marrow cells • Neural crest

ABSTRACT

We report the presence of neural crest-derived corneal precursors (COPs) that initiate spheres by clonal expansion from a single cell. COPs expressed the stem cell markers *nestin*, *Notch1*, *Musashi-1*, and *ABCG2* and showed the side population cell phenotype. COPs were multipotent with the ability to differentiate into adipocytes, chondrocytes, as well as neural cells, as shown by the expression of β-III-tubulin, glial fibrillary acidic protein, and neurofilament-M. COP spheres prepared from E/nestin-enhanced green fluorescent protein (EGFP) mice showed induction of EGFP expression that was not originally observed in the cornea, indicating activation of the neural-specific nestin second intronic enhancer in culture. COPs were Sca-1$^+$, CD34$^+$, CD45$^-$, and c-kit$^-$. Numerous GFP$^+$ cells were observed in the corneas of mice transplanted with whole bone marrow of transgenic mice ubiquitously expressing GFP; however, no GFP$^+$ COP spheres were initiated from these mice. On the other hand, COP spheres from transgenic mice encoding P0-Cre/Floxed-EGFP as well as Wnt1-Cre/Floxed-EGFP were GFP$^+$, indicating the neural crest origin of COPs, which was confirmed by the expression of the embryonic neural crest markers *Twist*, *Snail*, *Slug*, and *Sox9*. Taken together, these data indicate the existence of neural crest-derived, multipotent stem cells in the adult cornea. STEM CELLS *2006;24:2714–2722*

INTRODUCTION

The cornea is an avascular, structurally unique tissue that functions as the primary refracting medium of the eye. Although anatomically continuous with the vascularized sclera and conjunctiva, all three major components of the cornea function together to maintain optically clear tissue. Therefore, homeostasis of the corneal epithelium, stroma, and endothelium—the cellular components of the cornea—is vital in preserving transparency and optical precision.

Stem cell researchers of the cornea have identified the epithelial stem cell to be located in the vascular rim, or limbus, of the cornea [1]. In contrast, there is little evidence of the existence of stem/progenitor cells for keratocytes [2, 3], the resident cells of the corneal stroma. Keratocytes, mesenchymal cells distinct from keratinocytes of the skin, repopulate the corneal stroma during tissue remodeling after its depletion due to disease, such as herpes simplex virus infection, and trauma [4, 5]. Although the stroma of the cornea develops from the cranial neural crest [6, 7], the origin of keratocytes involved in the turnover of stromal tissue is unknown.

We have previously demonstrated that the neurosphere culture technique, which was originally developed for neural stem cells (NSCs) isolated from the forebrain of mouse [8], can be adapted to culture mouse cornea stromal cells for more than 15 passages while still maintaining the keratocyte phenotype [9]. A recent report demonstrated that multipotent precursor cells from adult mouse and human dermis, termed skin-derived precursor cells (SKPs), also form spheres and differentiate into neural and mesenchymal cells [10–12]. We therefore hypothesized that the corneal stroma-derived spheres we have isolated also include putative keratocyte precursor cells similar to SKPs of the skin.

Correspondence: Shigeto Shimmura, M.D., Department of Ophthalmology, Keio University School of Medicine, 35 Shinanomachi, Shinjuku-ku, Tokyo 160-8582, Japan. Telephone: +81-3-3353-1211; Fax: +81-3-3359-8302; e-mail: shige@sc.itc.keio.ac.jp; or Hideyuki Okano, M.D., Ph.D., Department of Physiology, Keio University School of Medicine, 35 Shinanomachi, Shinjuku-ku, Tokyo 160-8582, Japan. Telephone: +81-3-3353-1211; Fax: +81-3-3357-5445; e-mail: hidokano@sc.itc.keio.ac.jp Received March 16, 2006; accepted for publication July 24, 2006; first published online in STEM CELLS *EXPRESS* August 3, 2006. 1066-5099/2006/$20.00/0 doi: 10.1634/stemcells.2006-0156

Table 1. Polymerase chain reaction primers

Gene		Primer sequence (5′–3′)	Product size (bp)	GenBank accession ID
Abcg2	Forward:	CCATAGCCACAGGCCAAAGT	327	NM_011920
	Reverse:	GGGCCACATGATTCTTCCAC		
Nestin	Forward:	AATGGGAGGATGGAGAATGGAC	496	NM_016701
	Reverse:	TAGACAGGCAGGGCTAAGCAAG		
Musashi1	Forward:	GGCTTCGTCACTTTCATGGACC	542	NM_008629
	Reverse:	GGGAACTGGTAGGTGTAACCAG		
Notch1	Forward:	TGCCTGTGCACACCATCCTGC	247	NM_008714
	Reverse:	CAATCAGAGATGTTGGAATGC		
Twist	Forward:	CCAGAGAAGGAGAAAATGGACAGTC	259	NM_011658
	Reverse:	AAAAAGTGGGGTGGGGGGACACAAAC		
Snail	Forward:	CCCACTCGGATGTGAAGAGATACC	534	NM_011427
	Reverse:	ATGTGTCCAGTAACCACCCTGCTG		
Slug	Forward:	CACACACACACACACACACACACAG	570	NM_011415
	Reverse:	TGTCTTTCCCTCCTCTTCCAAGG		
Sox9	Forward:	CGCCCATCACCCGCTCGCAATACG	545	NM_011448
	Reverse:	AAGCCCCTCCTCGCTGATACTGG		
Mpz	Forward:	TTCCTGCTCTCCCTTTCCTACC	422	NM_008623
	Reverse:	CCTTTCCTTCCCATTCTCGC		
Gapd	Forward:	GACCACAGTCCATGCCATCAC	453	NM_008084
	Reverse:	TCCACCACCCTGTTGCTGTAG		

Here, we show the existence of multipotent keratocyte precursor cells (termed COPs, for cornea-derived precursors) in cornea stromal spheres isolated from adult mice. Single cells dissociated from spheres initiated clonal growth of progeny spheres, and a subset of COPs exhibited the side population (SP) cell phenotype. We sought to determine whether COPs were of bone marrow (BM) origin or of neural crest lineage by initiating COP spheres in various transgenic mice.

Materials and Methods

Animals

Normal, specific pathogen-free, adult C57BL/6J mice were purchased from CLEA Japan, Inc., Tokyo, http://www.clea-japan.com/index.html). Green fluorescent protein (GFP) transgenic mice (C57BL/6 TgN [act-enhanced GFP (EGFP)] OsbC14-Y01-FM131) were obtained from the Genome Information Research Center (Osaka University, Osaka, http://www.gen-info.osaka-u.ac.jp/welcome_en.html). Transgenic mice expressing Cre recombinase under the control of the Wnt1 promoter/enhancer (Wnt1-Cre mice) [13] and P0 promoter (P0-Cre mice) [14] were mated to CAG-CAT$^{loxP/loxP}$-EGFP (CAG-CAT-EGFP) transgenic mice [15] to obtain Wnt1-Cre/CAG-CAT-EGFP (Wnt1-Cre/Floxed-EGFP) and P0-Cre/CAG-CAT-EGFP (P0-Cre/Floxed-EGFP) transgenic mice, respectively. P0-Cre transgenic mice and CAG-CAT$^{loxP/loxP}$-EGFP transgenic mice were obtained from Dr. Ken-ichi Yamamura and Dr. Jun-ichi Miyazaki, respectively. All animal procedures were performed in accordance with institutional guidelines.

Cell Culture

Cells were dissociated from adult C57BL6/J mice and then cultured as described previously [9]. All animals were handled in full accordance with the ARVO (Association for Research in Vision and Ophthalmology) Statement for the Use of Animals in Ophthalmic and Vision Research. In brief, corneal stromal discs were cut into small pieces and digested in 0.05% trypsin (Sigma-Aldrich, St. Louis, http://www.sigmaaldrich.com) for 30 minutes at 37°C, followed by 78 U/ml collagenase (Sigma-Aldrich) and 38 U/ml hyaluronidase (Sigma-Aldrich) treatment for 30 minutes at 37°C. Stromal cells were mechanically dissociated into single cells and cultured in Dulbecco's modified Eagle's medium (DMEM)/F-12 (1:1) supplemented with 20 ng/ml epidermal growth factor (EGF) (Sigma-Aldrich), 10 ng/ml fibroblastic growth factor 2 (FGF2) (Sigma-Aldrich), B27 supplement (Invitrogen, Carlsbad, CA, http://www.invitrogen.com), and 10^3 U/ml leukemia inhibitory factor (Chemicon International, Temecula, CA, http://www.chemicon.com) at a density of 1×10^5 cells per milliliter at 37°C, 5% CO_2.

For clonal sphere expansion, COPs were initiated from corneas of wild-type C57BL/6 strain and transgenic strain expressing GFP ubiquitously [16]. Cells dissociated from COPs were plated on six-well dishes at a cell density of 5×10^3 cells per milliliter and cultured for 6–7 days in DMEM/F-12 containing 0.8% methylcellulose with EGF, FGF2, and B27 supplement. The use of methyl cellulose in the clone culture of NSCs (neural spheres) is an established method reported by several groups [17–24].

To examine the expression of nestin in COPs, cells were prepared from transgenic mice carrying EGFP (Clontech, Mountain View, CA, http://www.clontech.com) under the control of the second intronic enhancer of the *nestin* gene, which acts selectively in neural stem/precursor cells (E/nestin-EGFP) [25]. To confirm the neural crest origin of COPs, corneal stromal cells were prepared from six corneas of neonatal (13 days) and three corneas of adult (8 weeks) P0-Cre/Floxed-EGFP mice, as well as from one cornea of an adult (10 weeks) Wnt1-Cre/Floxed-EGFP mouse and cultured as described above.

In Vitro Differentiation

To examine neural differentiation, COPs were dissociated into single cells and suspended at a cell density of 10 cells per milliliter. One-hundred microliters of the cell suspension was divided into 48-well culture plates, and only clonal spheres from single cells were subcultured and expanded. Clonal COPs were

plated and cultured on poly(L-ornithine)/laminin-coated Lab-Tek chamber slides (Nalge Nunc International, Rochester, NY, http://www.nalgenunc.com). For α-smooth muscle actin (α-SMA) expression, clonal cells were also plated on Lab-Tek chamber slides in transforming growth factor (TGF)-β-containing medium. For adipogenic or chondrogenic differentiation, dissociated COPs were cultured in differentiation-inducing medium (Cambrex Bio Science Walkersville, Inc., Walkersville, MD, http://www.cambrex.com) according to instructions provided by the manufacturer. To visualize adipogenic differentiation, cells were stained with oil red O (Sigma-Aldrich). Chondrogenic differentiation was observed by the expression of the specific markers collagen II and aggrecan analyzed by immunocytochemistry of cell pellets (see above). Results were expressed as mean ± SD.

Immunohistochemistry

Cultured cells and frozen-tissue sections were fixed with 4% paraformaldehyde (PFA) for 10 minutes at room temperature and then stained with the following antibodies: anti-Bcrp1 (1:250; R&D Systems, Minneapolis, http://www.rndsystems.com), anti-α-SMA (1:200; NeoMarkers, Fremont, CA, http://www.labvision.com), anti-collagen type II (1:40; Chemicon International), anti-aggrecan (1:40; Chemicon International), anti-Musashi-1 (Msi1) (1:500, clone 14H1) [26], anti-class III β-tubulin (1:100, R&D Systems), anti-glial fibrillary acidic protein (GFAP) (1:200; Chemicon International), and anti-neurofilament-M (NF-M) (1:500; Abcam, Cambridge, U.K., http://www.abcam.com). Immunohistochemistry for GFP was performed using an anti-GFP antibody (1:500; MBL, Nagoya, Japan, http://www.mbl.co.jp) in 10-μm frozen sections from eyes fixed in 2% PFA overnight at 4°C. Immunoreactivity of primary antibodies was visualized using secondary antibodies conjugated with fluorescein isothiocyanate or cyanine 3 (Jackson ImmunoResearch Laboratories, West Grove, PA, http://www.jacksonimmuno.com).

Reverse Transcription-Polymerase Chain Reaction

COPs and cells freshly dissociated from mouse corneal stroma were collected and immediately frozen in liquid N_2. cDNA was synthesized using a commercially available kit (Life Sciences, Inc., St. Petersburg, FL, http://www.lifesci.com) from total RNA prepared using RNeasy kit (Qiagen, Hilden, Germany, http://www1.qiagen.com). Primers used for *Abcg2*, *Notch1*, *nestin*, *Msi1*, *Twist*, *Snail*, *Slug*, *Sox9*, and *Gapd* are shown in Table 1 (supplemental online data). Polymerase chain reaction (PCR) was performed using GeneAmp 9700 (Applied Biosystems, Foster City, CA, http://www.appliedbiosystems.com).

Flow Cytometry

For Hoechst dye efflux assays, single cells dissociated from COP spheres were incubated with Hoechst 33342 dye (Dojindo Laboratories, Kumamoto, Japan, http://www.dojindo.com) for 60 minutes at 37°C in the presence or absence of 50 μM reserpine (Daiichi Pharmaceutical, Tokyo, http://www.daiichius.com). SP cells were gated using FACS Vantage (BD Biosciences Immunocytometry Systems, San Jose, CA, http://www.bdbiosciences.com) as described previously [27]. Surface marker expression was also analyzed by flow cytometry using antibodies for CD45, CD34, Sca-1, c-kit, and CD133 (eBioscience, San Diego, http://www.ebioscience.com). Isotype-matched immunoglobulin G was used as negative control.

BM Transplantation

Whole BM (WBM) cells (1×10^6 cells) were prepared from GFP-transgenic mice [16] and transplanted into the retro-orbital space of C57BL6/J recipient mice treated with a lethal dose (10.3 Gy) of irradiation. Eight weeks after transplantation, recipient mice were sacrificed, and corneal stromal cells were prepared for sphere culture. Cells from the transplanted animals and nonirradiated animals were then mixed and cultured as described above to assess WBM-derived cell contribution to COP sphere formation.

RESULTS

COPs Initiate Clonal Sphere Formation

Mouse corneal stromal-derived spheres were first prepared and cultured as described previously [9]. To determine whether spheres arise from single putative COPs or from aggregates of floating cells, we first performed the clonal sphere-forming assay [17]. As shown in Figure 1, homogeneous GFP-positive or -negative spheres were found 6 days after plating. More than 70% of spheres were homogenous; however, nonclonal spheres composed of GFP-positive and -negative cells were also observed. The same observation was made by Kawase et al. [17], who reported that SKPs may aggregate at an initial cell density of 1×10^3 cells per milliliter during sphere cultures. Clonal sphere formation was observed for several passages (P5), suggesting that COPs possess high "self-renewing" potential.

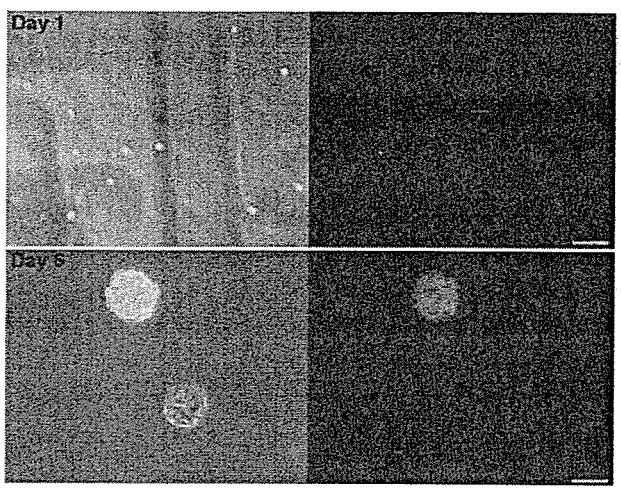

Figure 1. Single cornea-derived precursors form clonal spheres. Green fluorescent protein (GFP)-positive and -negative cells were mixed and cultured in methylcellulose-containing medium at a cell density of 5×10^3 cells per milliliter. Right and left panels show fluorescent images and phase-contrast images merged with fluorescent images, respectively. Upper panels show images of the cells 1 day after plating. After 6 days of culture, clonal spheres that consist entirely of GFP-positive or -negative cells were observed (lower panels). Scale bars = 200 μm (upper panel) and 100 μm (lower panel).

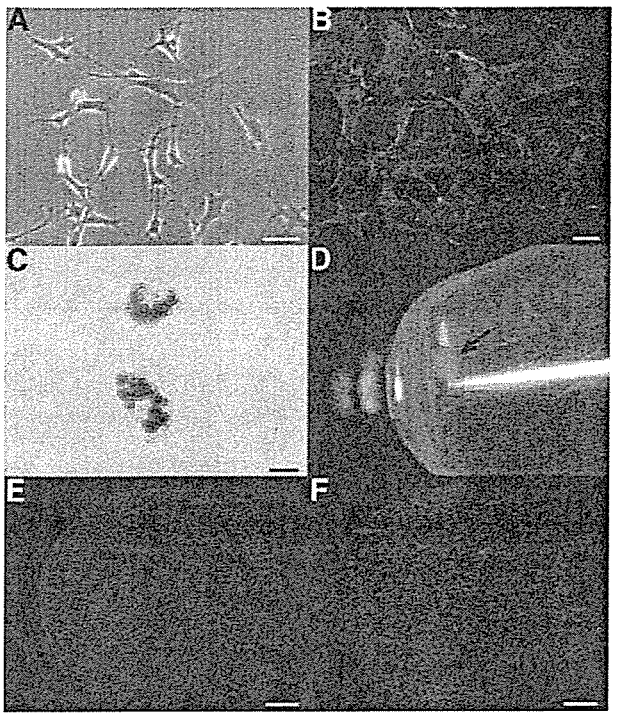

Figure 2. Cornea-derived precursors differentiate into mesenchymal cells. **(A):** Keratocyte phenotype in serum-free culture. **(B):** Anti-α-smooth muscle actin staining of myofibroblasts induced by transforming growth factor (TGF)-β. **(C):** Adipogenic cells stained with oil red O. Cells cultured in medium containing TGF-β3 formed chondrogenic pellets **(D)** (arrow) expressing collagen II **(E)** and aggrecan **(F)**. Scale bars = 50 μm **(A)**, 20 μm **(B, C)**, and 100 μm **(E, F)**.

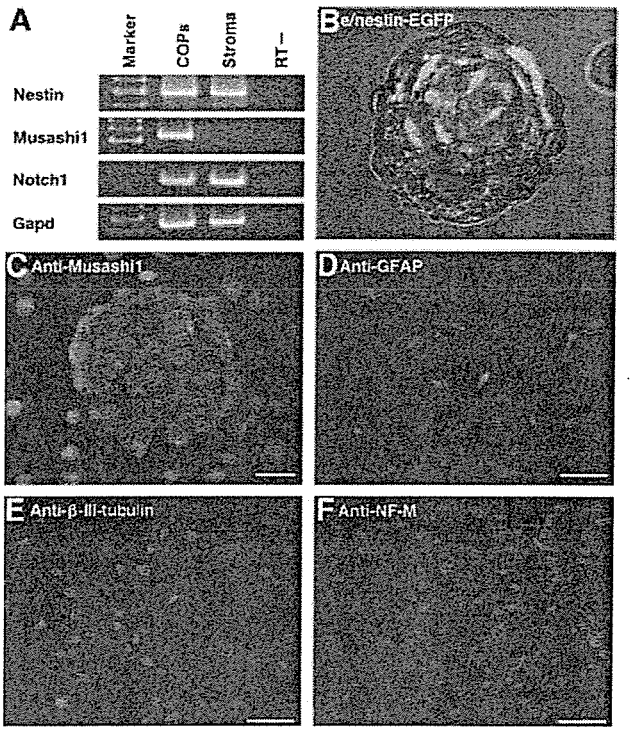

Figure 3. COP spheres express neural stem/precursor and differentiation markers. **(A):** Reverse transcription-polymerase chain reaction analysis of neural stem cell markers *Notch1*, *Musashi1*, and *nestin* expressed in COPs. *Gapd* was loaded as an internal control. **(B):** Fluorescent image merged with transmitted-light image of a COP sphere prepared from an E/nestin-EGFP mouse. EGFP expression confirms the activation of neuronal nestin. **(C):** Immunocytochemical analysis showed high levels of Musashi-1 expressed in COP spheres. Differentiated cells from COP spheres express the neuronal markers GFAP **(D)**, class III-β-tubulin **(E)**, and NF-M **(F)**. Cells were counterstained with 4,6-diamidino-2-phenylindole (blue) to show nuclei. Scale bars = 20 μm **(B, C)** and 50 μm **(D–F)**. Abbreviations: COP, cornea-derived precursor; EGFP, enhanced green fluorescent protein; GFAP, glial fibrillary acidic protein; NF-M, neurofilament-M; RT, reverse transcription.

COPs Differentiate into Neural and Mesenchymal Lineage Cells

COPs differentiate into keratocytes when cultured on plastic (Fig. 2A), into fibroblasts when cultured with serum, and into myofibroblasts under TGF-β stimulation (Fig. 2B) [9]. To determine whether these cells possess the ability to differentiate into other cells of mesenchymal lineage, COPs were cultured in various differentiation-inducing media. After 10 days of culture in medium containing insulin, approximately 7.9% (mean, $n = 2$) of the cells differentiated into oil red O-positive lipid-producing adipocytes (Fig. 2C). In addition, cell pellets were formed when cells were cultured in chondrogenic-inducing medium containing TGF-β3 ($n = 9$) (Fig. 2D). Immunofluorescent staining showed expression of the chondrocyte markers, type II collagen and aggrecan [28] in the pellets (Fig. 2E, 2F).

The NSC marker *Msi1*, an RNA-binding protein involved in the maintenance of NSCs and activation of Notch signaling [26, 29, 30], was expressed in COP spheres (Fig. 3A, 3C). COP spheres also expressed the NSC markers *nestin* [25, 31] and *Notch1* (Fig. 3A); the latter is a gene involved in the self-renewal of various types of tissue stem cells, including NSCs [32]. Because Nestin is an intermediate filament expressed by several cell types [33], COP spheres were prepared from E/nestin-EGFP transgenic mice, which carry the EGFP transgene under the control of a NSC-selective enhancer [25]. As expected, EGFP-positive spheres were formed (Fig. 3B) from these mice, which originally did not show EGFP-related fluorescence in the cornea.

Neural differentiation of COPs was shown by the expression of class III β-tubulin, GFAP, and NF-M in cells cultured on poly(L-ornithine)-coated slides in differentiation-inducing medium (Fig. 3E, 3F). Approximately 1.4% of cells stained with anti-NF-M antibody ($n = 3$), 36.9% ± 17.7% expressed GFAP ($n = 3$), and 32.8% ± 15.8% expressed β-III-tubulin ($n = 3$).

COP Spheres Are Rich in SP Cells

Several studies have shown that the ability to exclude Hoechst dye is a property of stem cells commonly referred to as SP cells [34], which are distinguished from the "main population" by flow cytometric analysis. The SP cell phenotype is defined by the dye exclusion ability of an ABC transporter, ABCG2, which is inhibited by ABC-transporter inhibitors such as reserpine. We found that COP spheres expressed ABCG2 when examined by reverse transcription (RT)-PCR and immunocytochemistry (Fig.

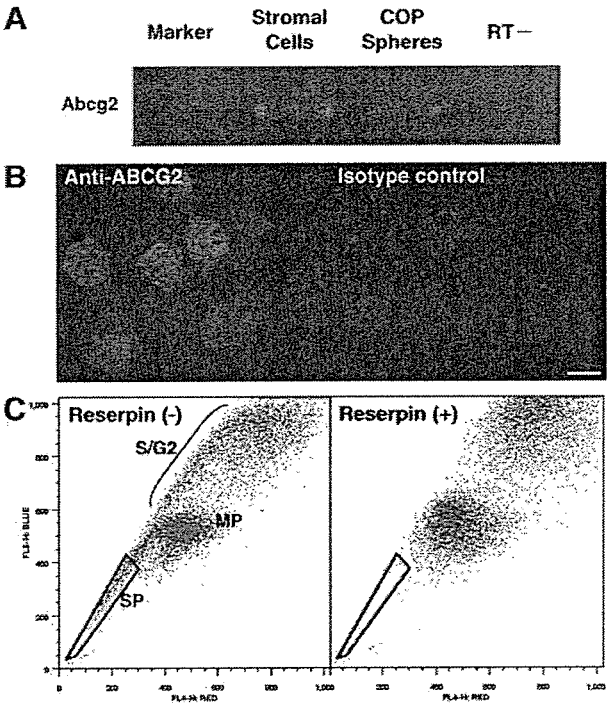

Figure 4. Murine COPs show ABCG2 expression and the SP cell phenotype. **(A):** RT-polymerase chain reaction analysis revealed *Abcg2* expression in COP spheres and in cells freshly dissociated from mouse corneal stroma. **(B):** Immunofluorescent staining of ABCG2 in COP spheres. Nuclei were counterstained with 4,6-diamidino-2-phenylindole. Scale bar = 100 μm. **(C):** Approximately 3.3% of sphere cells were SP cells as shown by flow cytometry. Hypofluorescent SP cells are distinct from MP cells and disappear when treated with reserpine, an inhibitor of ABCG2. Cells in the S/G_2 phase were not gated as SP cells, even though they disappeared with reserpine treatment. Abbreviations: COP, cornea-derived precursor; MP, main population; RT, reverse transcription; SP, side population.

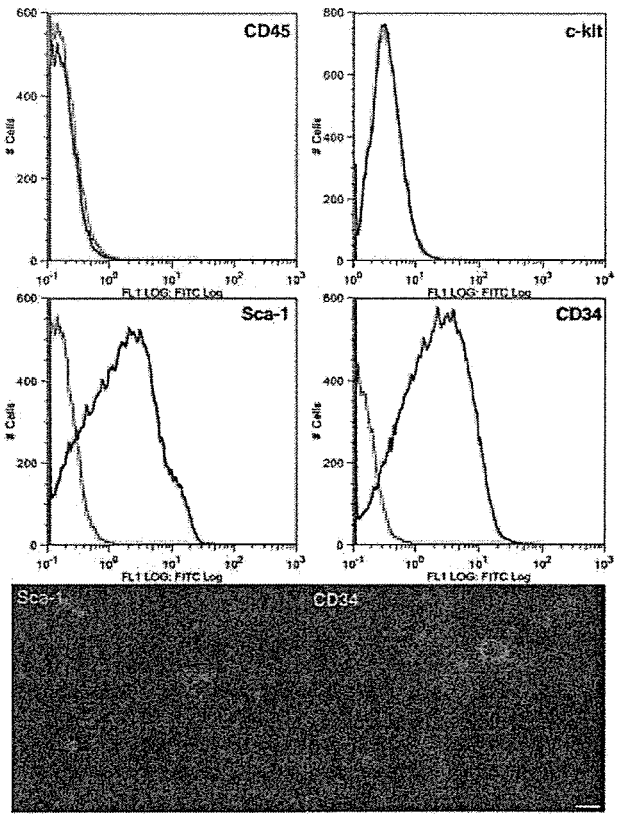

Figure 5. Cornea-derived precursors (COPs) express stem cell surface markers. **(A):** Single cells dissociated from COP spheres were stained with antibodies for CD45, c-kit, Sca-1, or CD34 and analyzed by flow cytometry (blue lines). Red lines represent isotype-matched negative control. COP sphere cells did not express CD45 or c-kit but did express Sca-1 and CD34. **(B):** Fluorescent images of cells stained with phycoerythrin-labeled anti-Sca-1 (left, red) or FITC-labeled anti-CD34 (right, green). Scale bar = 20 μm. Abbreviation: FITC, fluorescein isothiocyanate.

4A, 4B). Reserpine-sensitive SP cells were detected in dissociated sphere cells, representing 3.3% ± 1.2% (n = 8) of viable cells analyzed by flow cytometry (Fig. 4C).

We also analyzed several stem cell-related surface markers by flow cytometry. COP spheres expressed CD34 (Fig. 5A, 5B), a cell surface marker reported in rodent epithelial stem cells in the bulge area [35, 36], skeletal muscle stem cells [37, 38], and corneal stromal cells [9, 39]. In addition, expression of stem cell antigen-1 (Sca-1), a cell surface protein expressed in BM-derived hematopoietic stem cells (BM-HSCs) [40], mammary epithelial stem cells [41], a subpopulation of BM stromal cells [42], skeletal muscle stem cells [38], and SKP spheres [12], was found in 56.1% ± 19.2% (n = 7) of viable cells (Fig. 5). The expression of CD133, found in different types of primitive cells such as BM-HSCs, NSCs, and SKPs [43–46], was not observed (data not shown). Another cell surface marker, c-kit (CD117), the receptor for stem cell factor and a marker of BM-HSCs [47], was also not detected by flow cytometric analysis (Fig. 5) and RT-PCR (not shown).

COPs Are Neural Crest Lineage Cells

Although we found $CD34^+$ cells in COP spheres, Sosnova et al. [48] reported that all $CD34^+$ cells in mouse corneal stroma are $CD45^+$ BM-derived cells. In addition, the ability of BM-derived mesenchymal stem cells (BM-MSCs) to differentiate into multiple cell types has been reported [49, 50]. However, we found that COPs did not express CD45 (0.2% ± 0.2%, n = 6; Fig. 5A), indicating a nonhematopoietic origin for these cells. We further prepared COPs from mice transplanted with GFP^+ WBM cells. GFP^+ cells were not found in COP spheres prepared from the recipient mice 8 weeks after transplantation (Fig. 6C), although numerous GFP^+ cells were observed in the recipient cornea (Fig. 6A, 6B). GFP^+ cells in sphere culture preparations were found attached to the bottom of the culture dish, and immunofluorescent staining showed that the GFP^+ cells were $CD45^+$ and some also expressed CD34 (Fig. 6D). CD34 was therefore expressed in both BM-derived GFP^+ cells as well as GFP-COPs, indicating that WBM-derived cells are not likely to contribute to COP sphere-initiating cells.

Given that cranial neural crest-derived mesenchymal cells contribute to corneal stroma development, we next investigated whether COPs were of neural crest origin [6, 7]. COP spheres were prepared from Wnt1-Cre/Floxed-EGFP and P0-Cre/Floxed-EGFP transgenic mice in which neural crest-derived cells are tagged by EGFP expression [14, 51]. As expected, COP spheres prepared

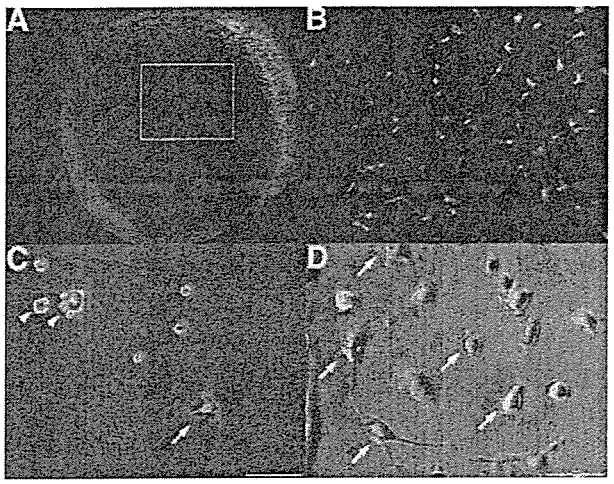

Figure 6. Bone marrow cells do not form cornea-derived precursor (COP) spheres. Sphere cultures prepared from C57BL6/J mice transplanted with whole bone marrow (WBM) cells of green fluorescent protein (GFP) mice did not produce GFP^+ spheres. **(A):** Fluorescent image of a cornea 8 weeks after WBM cell transplantation. Migration of numerous GFP^+ cells into the cornea was observed. **(B):** High-magnification view of the boxed area in **(A)**. **(C):** Phase-contrast image merged with fluorescent image of sphere culture at 7 days after plating. GFP^+ WBM-derived cells were found attached to the culture dish (arrow), whereas GFP^+ cells were not observed in forming spheres (arrowhead). **(D):** Adherent cells were stained with phycoerythrin-labeled anti-CD34 antibody (red). CD34 (arrows) was also expressed in transplanted WBM-derived cells (green). Scale bars = 200 μm **(C, D)**.

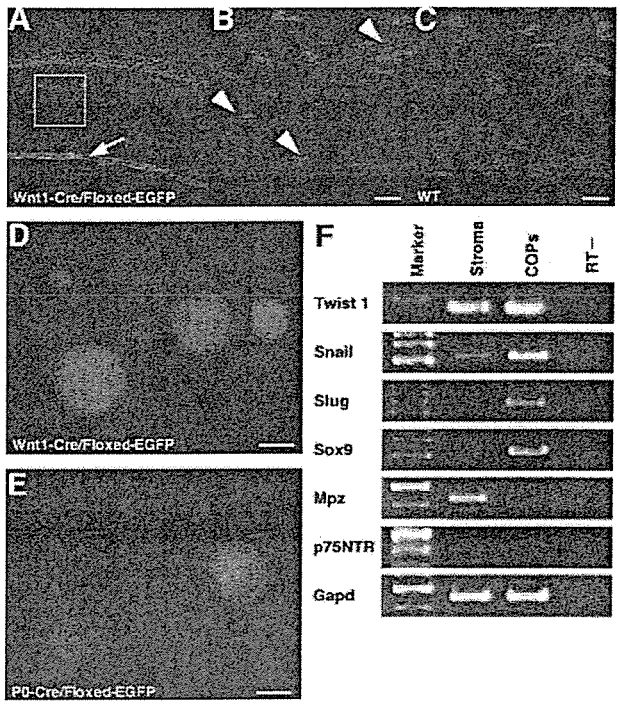

Figure 7. COPs are neural crest-derived cells. **(A–C):** Confocal images of Wnt1-Cre/Floxed-EGFP mouse **(A, B)** and WT mouse cornea **(C)** stained with anti-GFP antibody and cyanine 3-conjugated secondary antibody. **(B):** High-magnification view of the boxed region in **(A)**. Expression of EGFP is detected in keratocytes, although the expression level is low in vivo **(B)** (arrowheads). Positive staining is also detected in corneal endothelium, which is also neural crest-derived **(A)** (arrow). Cells dissociated from corneal stroma of Wnt1-Cre/Floxed-EGFP **(D)** (day 14) and P0-Cre/Floxed-EGFP mice **(E)** (day 6) formed $EGFP^+$ COP spheres. **(F):** Expression of embryonic neural crest markers by COPs and corneal stromal tissue. *Gapd* was loaded as an internal control. Expression of *Snail*, *Slug*, and *Sox9* was upregulated in COP spheres, whereas *Twist* was found in both COPs and stroma. *Mpz* was detected from stromal tissue only. Scale bars = 50 μm **(A, D, E)** and 20 μm **(B, C)**. Abbreviations: COP, cornea-derived precursor; EGFP, enhanced green fluorescent protein; GFP, green fluorescent protein; RT, reverse transcription; WT, wild-type.

from both transgenic mice were GFP^+ (Fig. 7D, 7E). To visualize GFP^+ neural crest-derived cells in the cornea, sections of Wnt1-Cre/Floxed-EGFP mouse were immunostained using anti-GFP antibody. Expression of GFP was detected in stromal keratocytes, although the expression level was low in vivo (Fig. 7B). Strong immunoreactivity was detected in the corneal endothelium (Fig. 7A), which are also neural crest-derived [52, 53]. We also examined embryonic neural crest-associated genes by RT-PCR analysis. *Twist*, *Slug*, *Snail*, and *Sox9* were expressed in COPs (Fig. 7F). These data confirm that COPs are neural crest-derived stem cells that are not recruited from the BM.

Discussion

The expansion of stem cells in vitro while maintaining properties of progenitor cells is critical from the standpoint of using stem cells for research as well as medical purposes. Culture conditions for several adult somatic stem cells, including BM-HSCs and NSCs, have been well-established. The sphere culture technique, which was originally developed for culturing NSCs as neurosphere from the central nervous system (CNS), was recently applied to isolate sphere-initiating cells from adult tissues other than CNS [2, 10–12, 17, 51, 54]. COPs have been subcultured for more than 13 months (more than 18 passages, corresponding to more than 90 population doublings) to date. As we discovered, not only do these cells have the ability to differentiate into keratocytes, fibroblasts, and myofibroblasts as observed in primary stromal keratocytes [9], COPs can also be induced to differentiate into adipocytes, chondrocytes, and neural cells.

Clonal spheres in this study were initiated using methylcellulose, which is an established method to clone hematopoietic cells and, more recently, embryonic stem cells and NCSs [17–24]. Cells within a sphere arising from a single cell were not necessarily homogeneous, which may be due to the position within a sphere or to autocrine and paracrine mechanisms. Dark cells in spheres (Fig. 1) were not GFP-negative but simply had low fluorescence under the conditions of our photography, which were set with exposure settings that do not cause saturation of fluorescent levels. This is vital because long exposure times can give the misleading impression of strong fluorescence in 100% of the cells, which is not the case.

We have also demonstrated that COPs include a high ratio of SP cells with Hoechst dye exclusion activity, which are regarded as a general property of progenitor-candidate cells. Although a higher percentage of cells seem to be ABCG2-positive by immunocytochemical analysis compared with flow cytometry, not all ABCG2-positive cells are drawn into the SP gate, which was defined by the inhibition of functional ABC transporters. Indeed, reserpine-sensi-

tive SP-like cells were found outside the SP gate, which may have been dividing cells exhibiting higher fluorescent intensity. The results of ABCG2 expression in COPs and the high fraction of SP cells suggest that the Hoechst dye exclusion assay may be used to further characterize COPs. A recent study by Du et al. also demonstrated the presence of SP cells in the human peripheral corneal stroma, which were shown to express neural and cartilage markers in addition to keratocyte markers [55]. We have confirmed that COP SP cells re-formed spheres after cell sorting (data not shown).

Other stem cell-related markers, including *nestin*, *Notch1*, and *Msi1*, were also expressed in COP spheres. Although the upregulation of Nestin is often used as evidence of a NSC phenotype, expression of this intermediate filament protein in non-neuronal cells has also been reported [56]. We therefore prepared COP spheres from transgenic mice carrying EGFP under the control of a neural-selective enhancer of the *nestin* gene [57–59]. Given that no fluorescence was observed in corneas of these mice, expression of nestin in corneal stromal cells revealed by RT-PCR analysis is probably due to non-neuronal expression. However, the fluorescence observed in COPs prepared from E/nestin-EGFP transgenic mice suggests that the neural stem/progenitor cell-specific enhancer was activated. Interestingly, we also found that expression of *Msi1* was upregulated only in COPs but not in the corneal stroma of the original mice. Recent reports demonstrated that Msi1 is expressed by epithelial stem cells in intestine [60, 61] and mammary gland [62], making Msi1 a candidate marker of adult stem cells in a variety of tissue sources.

There are only a limited number of reports describing putative progenitor cells for corneal keratocytes [2, 3]. Stromal keratocytes develop from mesenchymal cells originating in the cranial neural crest [6, 7]. A recent study demonstrated that late embryonic keratocytes maintain plasticity to differentiate into other neural crest-derived tissue when transplanted into embryos [63]. On the other hand, several reports have shown that BM-derived cells migrate to the corneal stroma [64, 65]. Recently, Sosnova et al. [48] reported that keratocytes do not express CD34 in the mouse corneal stroma and that all $CD34^+$ cells coexpressed CD45 and were therefore BM-derived. However, Espana et al. [39] reported CD34 expression in cultured human keratocytes. We found $CD34^+CD45^-$ cells in COP spheres (Fig. 5), which were distinct from the $CD34^+CD45^+$ adhesive cells isolated from corneas of GFP^+ WBM transplanted mice (Fig. 6). Given that GFP^+ COP spheres were not observed in GFP^+ WBM transplanted mice, COPs appear to be non-BM progenitors that express CD34, at least during sphere cultures. Furthermore, COPs prepared from Wnt1-Cre/Floxed-EGFP and P0-Cre/Floxed-EGFP mice were $EGFP^+$ (Fig. 7), strongly suggesting that these cells prepared from the cornea are of neural crest origin. Anti-GFP immunostaining also revealed neural crest-derived cells in the corneal stroma of Wnt1-Cre/Floxed-EGFP mice, with weaker levels of GFP expression in the stroma (Fig. 7B) compared with the endothelium (Fig. 7A). The weak expression of GFP in the stroma is probably due to the thin dendritic morphology of keratocytes, as well as the fact that stromal keratocytes are quiescent in vivo [66–68].

Further investigations are required to determine whether COPs are unique cells that reside in the corneal stroma or whether they represent a lineage of NSCs common with SKPs that migrate to the cornea. Although there is still controversy as to the identity of SKPs [69], the similarity of COPs with SKPs also has several clinical implications for the possible use of dermal cells for reconstructing the corneal stroma. If abundant dermal SKPs can be induced to differentiate into keratocytes, the development of corneal equivalents using autologous tissue may become a reality. Further studies to isolate COPs from humans for regenerative purposes are under way.

ACKNOWLEDGMENTS

We thank Kimie Kato for technical assistance, Hiroko Kouike for expert assistance with flow cytometric analysis, Fumito Morito for cell cultures, and Prof. Masaru Okabe (Genome Information Research Center) for providing the GFP-transgenic mice (C57BL/6 TgN [act-EGFP]OsbC14-Y01-FM131). This study was partly supported by a grant from the Advanced and Innovational Research Program in Life Sciences from the Ministry of Education, Culture, Sports, Science and Technology of Japan (to T.K. and H.O.), a grant from Core Research for Evolutional Science and Technology (CREST) of Japan Science and Technology Corporation (to H.O.), and a grant-in-aid to Keio University from the 21st Century Center of Excellence (COE) program.

DISCLOSURES

The authors indicate no potential conflicts of interest.

REFERENCES

1 Lavker RM, Tseng SC, Sun TT. Corneal epithelial stem cells at the limbus: Looking at some old problems from a new angle. Exp Eye Res 2004;78:433–446.

2 Uchida S, Yokoo S, Yanagi Y et al. Sphere formation and expression of neural proteins by human corneal stromal cells in vitro. Invest Ophthalmol Vis Sci 2005;46:1620–1625.

3 Funderburgh ML, Du Y, Mann MM et al. PAX6 expression identifies progenitor cells for corneal keratocytes. FASEB J 2005;19: 1371–1373.

4 Wilson SE, Pedroza L, Beuerman R et al. Herpes simplex virus type-1 infection of corneal epithelial cells induces apoptosis of the underlying keratocytes. Exp Eye Res 1997;64:775–779.

5 Helena MC, Baerveldt F, Kim WJ et al. Keratocyte apoptosis after corneal surgery. Invest Ophthalmol Vis Sci 1998;39:276–283.

6 Johnston MC, Noden DM, Hazelton RD et al. Origins of avian ocular and periocular tissues. Exp Eye Res 1979;29:27–43.

7 Trainor PA, Tam PP. Cranial paraxial mesoderm and neural crest cells of the mouse embryo: Co-distribution in the craniofacial mesenchyme but distinct segregation in branchial arches. Development 1995;121: 2569–2582.

8 Reynolds BA, Weiss S. Generation of neurons and astrocytes from isolated cells of the adult mammalian central nervous system. Science 1992;255:1707–1710.

9 Yoshida S, Shimmura S, Shimazaki J et al. Serum-free spheroid culture of mouse corneal keratocytes. Invest Ophthalmol Vis Sci 2005;46: 1653–1658.

10 Toma JG, McKenzie IA, Bagli D et al. Isolation and characterization of multipotent skin-derived precursors from human skin. STEM CELLS 2005;23:727–737.

11 Toma JG, Akhavan M, Fernandes KJ et al. Isolation of multipotent adult stem cells from the dermis of mammalian skin. Nat Cell Biol 2001;3: 778–784.

12 Fernandes KJ, McKenzie IA, Mill P et al. A dermal niche for multipotent adult skin-derived precursor cells. Nat Cell Biol 2004;6:1082–1093.

13 Danielian PS, Muccino D, Rowitch DH et al. Modification of gene activity in mouse embryos in utero by a tamoxifen-inducible form of Cre recombinase. Curr Biol 1998;8:1323–1326.

14 Yamauchi Y, Abe K, Mantani A et al. A novel transgenic technique that allows specific marking of the neural crest cell lineage in mice. Dev Biol 1999;212:191–203.

15 Kawamoto S, Niwa H, Tashiro F et al. A novel reporter mouse strain that expresses enhanced green fluorescent protein upon Cre-mediated recombination. FEBS Lett 2000;470:263–268.

16 Okabe M, Ikawa M, Kominami K et al. 'Green mice' as a source of ubiquitous green cells. FEBS Lett 1997;407:313–319.

17 Kawase Y, Yanagi Y, Takato T et al. Characterization of multipotent adult stem cells from the skin: Transforming growth factor-beta (TGF-beta) facilitates cell growth. Exp Cell Res 2004;295:194–203.

18 Suslov ON, Kukekov VG, Ignatova TN et al. Neural stem cell heterogeneity demonstrated by molecular phenotyping of clonal neurospheres. Proc Natl Acad Sci U S A 2002;99:14506–14511.

19 Ignatova TN, Kukekov VG, Laywell ED et al. Human cortical glial tumors contain neural stem-like cells expressing astroglial and neuronal markers in vitro. Glia 2002;39:193–206.

20 Laywell ED, Rakic P, Kukekov VG et al. Identification of a multipotent astrocytic stem cell in the immature and adult mouse brain. Proc Natl Acad Sci U S A 2000;97:13883–13888.

21 Kukekov VG, Laywell ED, Suslov O et al. Multipotent stem/progenitor cells with similar properties arise from two neurogenic regions of adult human brain. Exp Neurol 1999;156:333–344.

22 Gritti A, Frolichsthal-Schoeller P, Galli R et al. Epidermal and fibroblast growth factors behave as mitogenic regulators for a single multipotent stem cell-like population from the subventricular region of the adult mouse forebrain. J Neurosci 1999;19:3287–3297.

23 Kukekov VG, Laywell ED, Thomas LB et al. A nestin-negative precursor cell from the adult mouse brain gives rise to neurons and glia. Glia 1997;21:399–407.

24 Keller G, Kennedy M, Papayannopoulou T et al. Hematopoietic commitment during embryonic stem cell differentiation in culture. Mol Cell Biol 1993;13:473–486.

25 Kawaguchi A, Miyata T, Sawamoto K et al. Nestin-EGFP transgenic mice: Visualization of the self-renewal and multipotency of CNS stem cells. Mol Cell Neurosci 2001;17:259–273.

26 Kaneko Y, Sakakibara S, Imai T et al. Musashi1: An evolutionally conserved marker for CNS progenitor cells including neural stem cells. Dev Neurosci 2000;22:139–153.

27 Murayama A, Matsuzaki Y, Kawaguchi A et al. Flow cytometric analysis of neural stem cells in the developing and adult mouse brain. J Neurosci Res 2002;69:837–847.

28 Shukunami C, Shigeno C, Atsumi T et al. Chondrogenic differentiation of clonal mouse embryonic cell line ATDC5 in vitro: Differentiation-dependent gene expression of parathyroid hormone (PTH)/PTH-related peptide receptor. J Cell Biol 1996;133:457–468.

29 Sakakibara S, Nakamura Y, Yoshida T et al. RNA-binding protein Musashi family: Roles for CNS stem cells and a subpopulation of ependymal cells revealed by targeted disruption and antisense ablation. Proc Natl Acad Sci U S A 2002;99:15194–15199.

30 Sakakibara S, Okano H. Expression of neural RNA-binding proteins in the postnatal CNS: Implications of their roles in neuronal and glial cell development. J Neurosci 1997;17:8300–8312.

31 Sawamoto K, Yamamoto A, Kawaguchi A et al. Direct isolation of committed neuronal progenitor cells from transgenic mice coexpressing spectrally distinct fluorescent proteins regulated by stage-specific neural promoters. J Neurosci Res 2001;65:220–227.

32 Reya T, Morrison SJ, Clarke MF et al. Stem cells, cancer, and cancer stem cells. Nature 2001;414:105–111.

33 Kobayashi M, Sjoberg G, Soderhall S et al. Pediatric rhabdomyosarcomas express the intermediate filament nestin. Pediatr Res 1998;43: 386–392.

34 Staud F, Pavek P. Breast cancer resistance protein (BCRP/ABCG2). Int J Biochem Cell Biol 2005;37:720–725.

35 Blanpain C, Lowry WE, Geoghegan A et al. Self-renewal, multipotency, and the existence of two cell populations within an epithelial stem cell niche. Cell 2004;118:635–648.

36 Morris RJ, Liu Y, Marles L et al. Capturing and profiling adult hair follicle stem cells. Nat Biotechnol 2004;22:411–417.

37 Jackson KA, Mi T, Goodell MA. Hematopoietic potential of stem cells isolated from murine skeletal muscle. Proc Natl Acad Sci U S A 1999; 96:14482–14486.

38 Torrente Y, Tremblay JP, Pisati F et al. Intraarterial injection of muscle-derived CD34(+)Sca-1(+) stem cells restores dystrophin in mdx mice. J Cell Biol 2001;152:335–348.

39 Espana EM, Kawakita T, Liu CY et al. CD-34 expression by cultured human keratocytes is downregulated during myofibroblast differentiation induced by TGF-beta1. Invest Ophthalmol Vis Sci 2004;45:2985–2991.

40 Ito CY, Li CY, Bernstein A et al. Hematopoietic stem cell and progenitor defects in Sca-1/Ly-6A-null mice. Blood 2003;101:517–523.

41 Welm BE, Tepera SB, Venezia T et al. Sca-1(pos) cells in the mouse mammary gland represent an enriched progenitor cell population. Dev Biol 2002;245:42–56.

42 Satoh M, Mioh H, Shiotsu Y et al. Mouse bone marrow stromal cell line MC3T3-G2/PA6 with hematopoietic-supporting activity expresses high levels of stem cell antigen Sca-1. Exp Hematol 1997;25:972–979.

43 Richardson GD, Robson CN, Lang SH et al. CD133, a novel marker for human prostatic epithelial stem cells. J Cell Sci 2004;117:3539–3545.

44 Corbeil D, Roper K, Hellwig A et al. The human AC133 hematopoietic stem cell antigen is also expressed in epithelial cells and targeted to plasma membrane protrusions. J Biol Chem 2000;275:5512–5520.

45 Uchida N, Buck DW, He D et al. Direct isolation of human central nervous system stem cells. Proc Natl Acad Sci U S A 2000;97:14720–14725.

46 Belicchi M, Pisati F, Lopa R et al. Human skin-derived stem cells migrate throughout forebrain and differentiate into astrocytes after injection into adult mouse brain. J Neurosci Res 2004;77:475–486.

47 Jackson KA, Majka SM, Wulf GG et al. Stem cells: A minireview. J Cell Biochem Suppl 2002;38:1–6.

48 Sosnova M, Bradl M, Forrester JV. $CD34^+$ corneal stromal cells are bone marrow-derived and express hemopoietic stem cell markers. STEM CELLS 2005;23:507–515.

49 Hermann A, Gastl R, Liebau S et al. Efficient generation of neural stem cell-like cells from adult human bone marrow stromal cells. J Cell Sci 2004;117:4411–4422.

50 Anjos-Afonso F, Siapati EK, Bonnet D. In vivo contribution of murine mesenchymal stem cells into multiple cell-types under minimal damage conditions. J Cell Sci 2004;117:5655–5664.

51 Tomita Y, Matsumura K, Wakamatsu Y et al. Cardiac neural crest cells contribute to the dormant multipotent stem cell in the mammalian heart. J Cell Biol 2005;170:1135–1146.

52 Cvekl A, Tamm ER. Anterior eye development and ocular mesenchyme: New insights from mouse models and human diseases. Bioessays 2004; 26:374–386.

53 Gage PJ, Rhoades W, Prucka SK et al. Fate maps of neural crest and mesoderm in the mammalian eye. Invest Ophthalmol Vis Sci 2005;46: 4200–4208.

54 Molofsky AV, Pardal R, Iwashita T et al. Bmi-1 dependence distinguishes neural stem cell self-renewal from progenitor proliferation. Nature 2003;425:962–967.

55 Du Y, Funderburgh ML, Mann MM et al. Multipotent stem cells in human corneal stroma. STEM CELLS 2005;23:1266–1275.

56 Wroblewski J, Engstrom M, Edwall-Arvidsson C et al. Distribution of nestin in the developing mouse limb bud in vivo and in micro-mass cultures of cells isolated from limb buds. Differentiation 1997;61: 151–159.

57 Mignone JL, Kukekov V, Chiang AS et al. Neural stem and progenitor cells in nestin-GFP transgenic mice. J Comp Neurol 2004;469:311–324.

58 Zimmerman L, Parr B, Lendahl U et al. Independent regulatory elements in the nestin gene direct transgene expression to neural stem cells or muscle precursors. Neuron 1994;12:11–24.

59 Lothian C, Lendahl U. An evolutionarily conserved region in the second intron of the human nestin gene directs gene expression to CNS progenitor cells and to early neural crest cells. Eur J Neurosci 1997;9:452–462.

60 Kayahara T, Sawada M, Takaishi S et al. Candidate markers for stem and early progenitor cells, Musashi-1 and Hes1, are expressed in crypt base columnar cells of mouse small intestine. FEBS Lett 2003;535:131–135.

61 Potten CS, Booth C, Tudor GL et al. Identification of a putative intestinal stem cell and early lineage marker; musashi-1. Differentiation 2003;71: 28–41.

62 Clarke RB, Spence K, Anderson E et al. A putative human breast stem cell population is enriched for steroid receptor-positive cells. Dev Biol 2005;277:443–456.

63 Lwigale PY, Cressy PA, Bronner-Fraser M. Corneal keratocytes retain neural crest progenitor cell properties. Dev Biol 2005;288:284–293.

64 Nakamura T, Ishikawa F, Sonoda KH et al. Characterization and distribution of bone marrow-derived cells in mouse cornea. Invest Ophthalmol Vis Sci 2005;46:497–503.

65 Hamrah P, Liu Y, Zhang Q et al. The corneal stroma is endowed with a significant number of resident dendritic cells. Invest Ophthalmol Vis Sci 2003;44:581–589.

66 Beales MP, Funderburgh JL, Jester JV et al. Proteoglycan synthesis by bovine keratocytes and corneal fibroblasts: Maintenance of the keratocyte phenotype in culture. Invest Ophthalmol Vis Sci 1999;40: 1658–1663.

67 Jester JV, Barry PA, Lind GJ et al. Corneal keratocytes: In situ and in vitro organization of cytoskeletal contractile proteins. Invest Ophthalmol Vis Sci 1994;35:730–743.

68 West-Mays JA, Dwivedi DJ. The keratocyte: Corneal stromal cell with variable repair phenotypes. Int J Biochem Cell Biol 2006;38:1625–1631.

69 Rendl M, Lewis L, Fuchs E. Molecular dissection of mesenchymal-epithelial interactions in the hair follicle. PLoS Biol 2005;3:e331.

See www.StemCells.com for supplemental material available online.

Proliferation and Differentiation of Transplantable Rabbit Epithelial Sheets Engineered with or without an Amniotic Membrane Carrier

Kazunari Higa,[1] *Shigeto Shimmura,*[1,2] *Naoko Kato,*[2] *Tetsuya Kawakita,*[1] *Hideyuki Miyashita,*[2] *Yuji Itabashi,*[3] *Keiichi Fukuda,*[3] *Jun Shimazaki,*[1,2] *and Kazuo Tsubota*[1,2]

PURPOSE. To report a novel method of engineering transplantable, carrier-free corneal epithelial sheets by using a biodegradable fibrin sealant and to compare its characteristics with epithelial sheets cultivated on denuded amniotic membrane carriers.

METHODS. Stratified corneal epithelial sheets were prepared in culture dishes coated with biodegradable fibrin glue. Amniotic membrane (AM) carriers served as the control. The quality of cultivated sheets was compared by immunohistochemistry for cytokeratin (K)3, K12, K14, p63, occludin, and integrin β1; electron microscopy; and colony-forming assays. K3 protein expression was compared by Western blot analysis. In a limbal-deficient rabbit transplantation model, postoperative adaptation and proliferation of BrdU-labeled cell sheets were examined by histology and anti-Ki67 staining.

RESULTS. Epithelial sheets were successfully engineered by using a biodegradable fibrin sealant. Cell sheets in both groups were multilayered, expressed K3, K12, and K14, and had functioning occludin$^+$ apical tight junctions as well as p63 and integrin β1 staining in basal cells. The carrier-free sheets appeared to be more differentiated than the AM sheets, which was also demonstrated by the higher levels of K3 in the Western blots. The colony-forming efficiency of dissociated cells was similar in both groups, although larger colonies were observed on the AM sheets. AM sheets retained higher levels of BrdU-labeled cells and fewer Ki67$^+$ cells compared with carrier-free sheets after transplantation.

CONCLUSIONS. Tissue engineering with a commercially available fibrin sealant was an effective means of creating a carrier-free, transplantable corneal epithelial sheet. Carrier-free sheets were more differentiated compared with AM sheets, while retaining similar levels of colony-forming progenitor cells. (*Invest Ophthalmol Vis Sci.* 2007;48:597–604) DOI:10.1167/iovs.06-0664

From the [1]Department of Ophthalmology, Tokyo Dental College, Chiba, Japan; and the Departments of [2]Ophthalmology and [3]Regenerative Medicine and Advanced Cardiac Therapeutics, Keio University School of Medicine, Tokyo, Japan.

Supported in part by a grant from Advanced and Innovational Research Program in Life Sciences from the Ministry of Education, Culture, Sports, Science and Technology (TK) and a Grant-in-Aid for Scientific Research (SS).

Submitted for publication June 15, 2006; revised September 22, 2006; accepted December 14, 2006.

Disclosure: **K. Higa**, None; **S. Shimmura**, None; **N. Kato**, None; **T. Kawakita**, None; **H. Miyashita**, None; **Y. Itabashi**, None; **K. Fukuda**, None; **J. Shimazaki**, None; **K. Tsubota**, None

The publication costs of this article were defrayed in part by page charge payment. This article must therefore be marked "*advertisement*" in accordance with 18 U.S.C. §1734 solely to indicate this fact.

Corresponding author: Shigeto Shimmura, Department of Ophthalmology, Keio University School of Medicine, 35 Shinanomachi, Shinjuku-ku, Tokyo 160-8582, Japan; shige@sc.itc.keio.ac.jp.

The use of allogenic or autologous cell sources for regenerative surgery is already common practice in the reconstruction of the ocular surface in patients with stem cell deficiency.[1,2] After the success of limbal transplantation, a second generation of regenerative corneal surgery has emerged in the form of cell sheet transplantation by tissue-engineering techniques.[3] Cell sheet transplants currently in clinical use are prepared by using biological carriers such as fibrin[4] or amniotic membrane (AM)[5–7] or as carrier-free cell sheets.[8,9] Although there is still debate as to whether the cultivated sheets include progenitor or stem cells, both carrier and carrier-free techniques have restored a clear ocular surface for at least 1 year, the empiric goal for successful stem cell surgery.[7,9]

One of the major benefits of cell sheet transplants, is that it can avoid the problem of donor availability. In vitro expansion provides a stratified cell sheet suitable for transplantation from a millimeter-scale tissue source procured from the healthy eye of the same patient or from a living relative in the case of bilateral disease. Ectopic cell sources such as the buccal membrane can also be modified in vitro to form a stratified epithelial sheet for ocular surface reconstruction with autologous tissue.[9–11] Yet, the number of clinical cases has not met the needs of patients because of ethical and technical constraints. Using AM as a carrier is one possibility as a standardized technique to produce transplantable epithelial sheets; however, AM tissue may not be readily available.

The development of a carrier-free method to produce corneal epithelial sheets was first reported by Nishida et al.,[8] who used a novel temperature-responsive polymer that changes molecular conformation and hydrophobicity at 20°C to release intact sheets. Clinical cases in which this technique has been used have shown that a carrier-free strategy is feasible and that transplantation can be performed without the use of sutures. In the present study, we developed a different technique by using commercially available fibrin sealants to produce carrier-free sheets. Our method is different from the fibrin carrier sheets described by Rama et al.,[4] as we allowed the fibrin to be degraded by intrinsic proteases before transplantation.

MATERIALS AND METHODS

Antibodies

Mouse monoclonal antibodies (mAbs) for cytokeratin (K)3, K14, laminin, p63, integrin β1, and Ki67 were purchased from Progen (AE5; Heidelberg, German), Abcam (B4-29; Cambridgeshire, UK), Laboratory Vision (4C7; Fremont, CA), Calbiochem (4A4; Merck KGaA, Darmstadt, Germany), Chemicon International Inc. (LM534; Temecula, CA), and DakoCytomation (MIB-1; Glostrup, Denmark), respectively. Mouse IgM antibody for fibrin was purchased from Monosan (Uden, The Netherlands). Rabbit polyclonal antibody for K12, goat polyclonal antibody for type IV collagen and rat mAb for BrdU (ICR1) were purchased from TransGenic, Inc. (Kumamoto, Japan), Southern Biotechnology Associates, Inc. (Birmingham, AL) and Abcam. Isotype goat IgG, mouse IgG1,

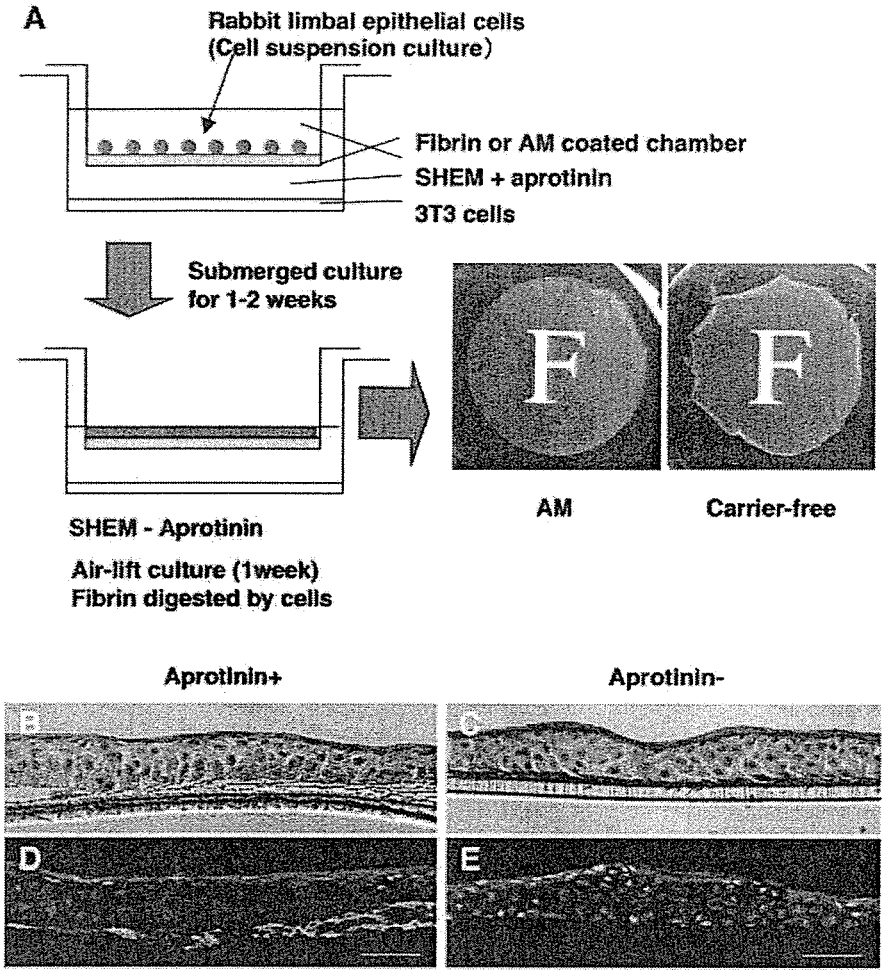

FIGURE 1. Cultivation of carrier-free epithelial sheets. Limbal epithelial cells were collected and seeded on fibrin- or AM-coated chambers (A). After 1 to 2 weeks in submerged culture with MMC-treated 3T3 feeder fibroblasts, the cells were allowed to stratify at the air–liquid interface for 1 week. HE staining (B, C) and immunohistochemistry against fibrin (*green*) and K12 (*red*) (D, E) showed that fibrin acted as a scaffold during cultivation with the protease inhibitor aprotinin (B, D) and was allowed to dissolve by removing the aprotinin before transplantation (C, E).

mouse IgM, rabbit IgG and rat IgG as control were purchased from Santa Cruz Biotechnology (Santa Cruz, CA), Dako Cytomation, and Jackson ImmunoResearch Laboratories (West Grove, PA), respectively. FITC-, rhodamine-, and Cy3-conjugated secondary antibodies were purchased from Jackson ImmunoResearch Laboratories and Chemicon International Inc.

Preparation of Epithelial Cells Sheets

All experimental procedures and protocols were approved by the Animal Care and Use Committee of Tokyo Dental College and conformed to the National Instituted of Health Guide for the Care and Use of Laboratory Animals. Fibrin sealant was purchased from Fujisawa (Bolheal; Osaka, Japan), and its constitution was performed as reported previously.[12] In brief, a solution containing 40 mg of human fibrinogen and 0.18 U of thrombin was diluted with 7.5 mL saline, and 0.3 mL was spread rapidly onto the upper chambers of a six-well plate with culture inserts (Transwell; Costar Corning, Corning, NY). Two hours later, the polymerized fibrin-coated top chambers were obtained and stored at 4°C. AMs were donated by mothers who were seronegative for human immunodeficiency virus and hepatitis B and C virus at the time of cesarean section, after written informed consent was obtained, in accordance with the Declaration of Helsinki. AM was stored with 15% dimethylsulfoxide (Sigma-Aldrich, St. Louis, MO) with PBS at −80°C until use. Denuded AM was prepared as previously described.[7] Membranes were rinsed in PBS, spread onto the upper chambers of a six-well insert, frozen at −80°C, and air-dried at room temperature.

Primary cultures of limbal epithelial cells were prepared from eyes of 2.5- to 3.0-kg female Japanese white rabbits (Japan CLEA, Tokyo, Japan) with anesthesia induced by intravenous injection of 4 mL pentobarbital sodium (50 mg/mL). Limbal rims of corneoscleral tissue were prepared by careful removal of excess sclera, iris, corneal endothelium, and central cornea. Epithelial sheets were isolated as described previously.[13] Dispersed epithelial sheets were treated with trypsin-ethylenediaminetetracetic acid (EDTA) for 10 minutes, to suspend cells, which were seeded onto fibrin- or AM-coated wells (2×10^5 cells/mL) with supplemented hormonal epithelial medium (SHEM)[7] containing 666 KIU/mL aprotinin (Wako, Osaka, Japan) and cocultured with mitomycin C (MMC)-treated 3T3 fibroblasts (Fig. 1A). The cultures were submerged in medium until confluence, cultured in air–liquid interface for 1 week, and finally incubated without aprotinin for 4 days. To evaluate the proliferation of transplanted epithelium and to identify cells of donor origin, cell sheets were labeled with 10 μM BrdU for 48 hours before surgery. After labeling with BrdU, the epithelial cell sheets were washed with fresh medium and then used for surgery.

Transmission Electron Microscopy

Epithelial cell sheets were processed for transmission electron microscopy. Epithelial cell sheets from both groups were fixed in 2.5% glutaraldehyde solution in 60 mM HEPES buffer solution for 4 hours. After washing, samples were postfixed in 1% osmium tetroxide, dehydrated in a series of ethanol and propylene oxide, and embedded in epoxy resin. Semithin sections (1-μm) were stained with toluidine blue. Then, ultrathin specimens were sectioned with a microtome (LKB, Gaithersburg, MD). Sections in the range of gray to silver were collected on 150-mesh grid, stained with uranyl acetate and lead

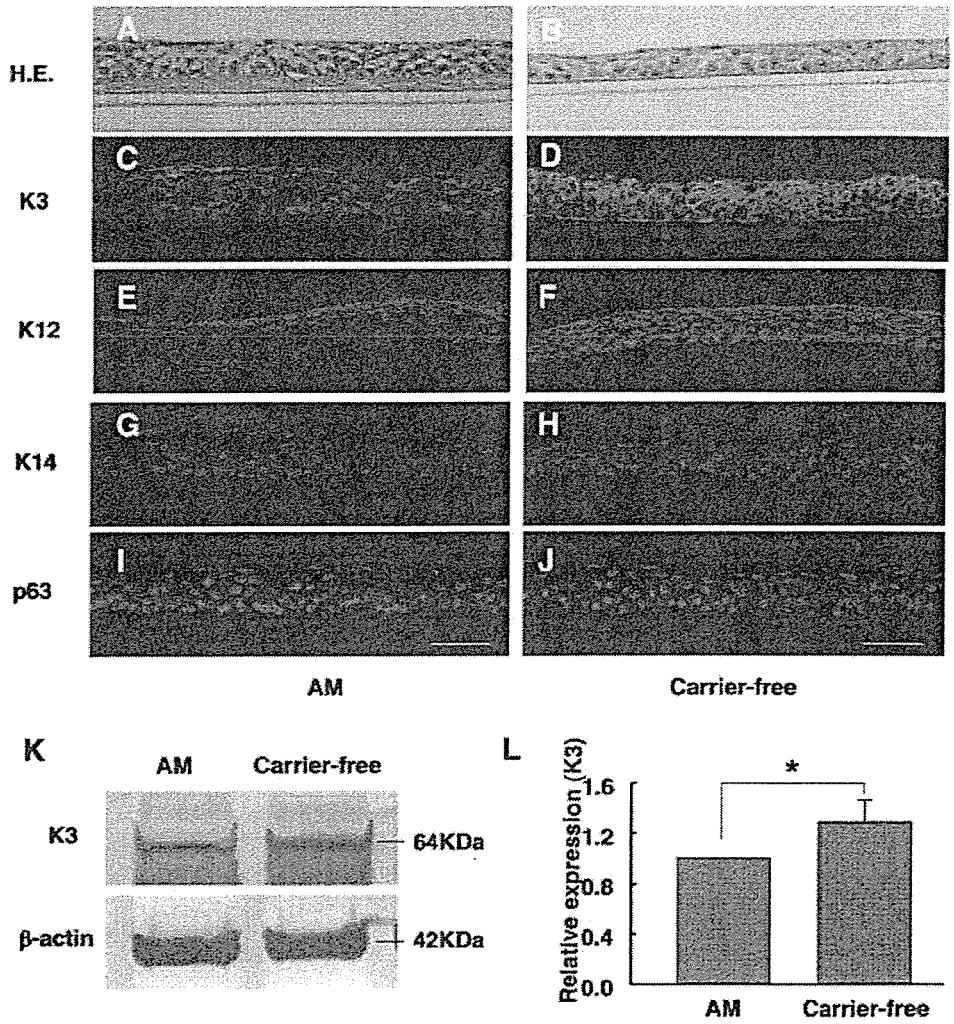

FIGURE 2. Differentiation markers in epithelial sheets. Hematoxylin and eosin staining of AM (**A**) and carrier-free (**B**) epithelial cell sheets. (**C**–**J**) Immunohistochemistry of K3, K12, K14, and p63 in epithelial sheets. Carrier-free sheets showed stronger K3/K12 staining and weaker K14/p63 staining than did AM sheets. Nuclei of cells were stained with DAPI. Scale bar, 50 μm. The difference in K3 expression was confirmed by Western blot (**K**), which showed significantly higher levels of K3 in carrier-free sheets than in AM sheets, when compared semiquantitatively (**L**, $n = 6$, $^*P = 0.002$).

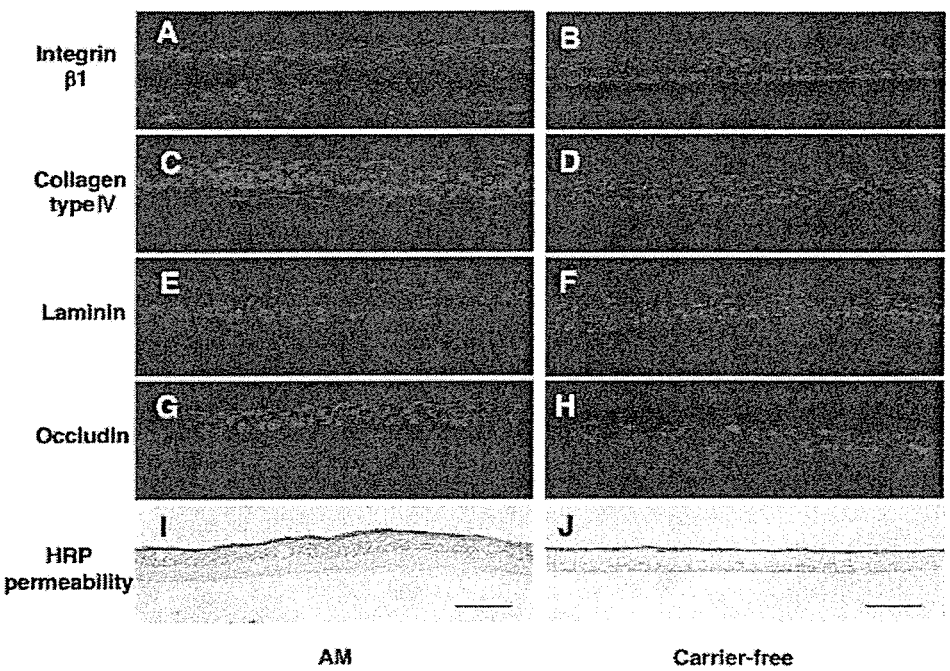

FIGURE 3. Basement membrane components and barrier function in epithelial sheets. Immunohistochemistry of integrin β1, collagen type IV, laminin, and occludin in AM (**A**, **C**, **E**, **G**) and carrier-free (**B**, **D**, **F**, **H**) epithelial sheets. Nuclei of cells were stained with DAPI. (**I**, **J**) Barrier function (HRP permeability) of the epithelial sheets. Scale bar, 50 μm.

citrate, and examined under an electron microscope (model 1200 EXII; JEOL, Tokyo, Japan).

Colony-Forming Efficiency

To evaluate the proliferative potential of cells in the cultured sheets, MMC-treated 3T3 fibroblasts were used in a colony-forming efficiency (CFE) assay, as previously described.[14–16] NIH 3T3 fibroblasts in DMEM containing 10% FCS were treated with MMC (4 μg/mL) for 2 hours at 37°C and then treated with trypsin-EDTA and plated at a density of 3×10^6 cells in 100-mm culture dishes. Single cells were prepared from both treated epithelial cell sheets (Acutase; Innovative Cell Technologies, Inc., San Diego, CA) for 60 minutes at 37°C. Each dish was seeded at 1×10^3 cells/dish. CFE was calculated by the percentage of colonies at day 14 generated by the number of epithelial cells plated in the dish. Quantification of size (in square millimeters) and number of colonies obtained from AM or fibrin sheets ($n = 5$) was performed by NIH Image (available by ftp at zippy.nimh.nih.gov/ or at http://rsb.info.nih.gov/nih-image; developed by Wayne Rasband, National Institutes of Health, Bethesda, MD). Growth capacity was evaluated on day 14 when cultured cells were stained with rhodamine B (Wako) for 30 minutes.

Epithelial Sheet Transplantation

All animals were handled in full accordance with the ARVO Statement for the Use of Animals in Ophthalmic and Vision Research and institutional guidelines. Rabbits were anesthetized with intramuscular injection of xylazine hydrochloride (2.5 mg/mL) and ketamine hydrochloride (37.5 mg/mL). The left eye in each rabbit was rendered totally limbal stem cell deficient by 1-*n*-heptanol (Sigma-Aldrich) mechanical debridement of the corneal epithelium, and surgical removal of the limbal and conjunctival epithelium was performed up to 2 mm from the limbus. Carrier-free sheets were gently detached from the mesh with a cell scraper,[12] transferred by microforceps and then expanded on the bare corneal stroma with a surgical sponge or forceps. Cell sheets were allowed to attach for 5 minutes without sutures. AM carrier sheets were sutured to the corneal surface with 10-0 nylon sutures. Rabbits with denuded corneas without sheet transplants served as the control. After surgery, all rabbits were fitted with a bandage contact lens and topical antibiotic (levofloxacin), and steroids (betamethasone) were applied twice daily.

The percentage of the cornea covered by epithelium at 1 week after surgery was calculated by measuring the area of the epithelial defects. The defect area was analyzed by tracing fluorescein images and calculated using the NIH Image program. Rabbits were then killed to observe BrdU-labeled cells as a means to confirm the donor origin of epithelium. The proliferation of transplanted epithelial cells was examined by calculating the percentage of $BrdU^+$ and $Ki67^+$ nuclei by immunohistochemistry.

Immunohistochemistry

Paraffin sections (K3, K14, p63, BrdU, and Ki67) were deparaffinized in xylene and rehydrated. Frozen sections (type IV collagen and laminin) were fixed for 10 minutes in cold acetone before blocking. Frozen sections (integrin β1 and K12) were fixed for 10 minutes in 2% paraformaldehyde (Wako). Sections were blocked by incubation with 10% normal donkey serum (Chemicon International Inc., Temecula, CA) and 1% bovine serum albumin (Sigma-Aldrich) for 1 hour at room temperature (RT). Antibodies to K3 (1:50), K12 (1:100), K14 (1:100), p63 (1:50), BrdU (1:100), Ki67 (1:50), type IV collagen (1:50), laminin (1:50), and integrin β1 (1:100) were applied and incubated for 90 minutes at RT, followed by incubation with rhodamine- or Cy3-conjugated secondary antibody. After three washes with TBST, the sections were incubated with 1 mg/mL 4′,6-diamidino-2-phenylindole (DAPI; Dojindo Laboratories, Tokyo, Japan) at RT for 5 minutes. Finally, the sections were washed three times in TBST and coverslipped after mounting with an antifade medium (50 mM Tris buffer saline, 90% glycerin; Wako), 10% 1,4-diazabicyclo-2,2,2-octane (Wako).

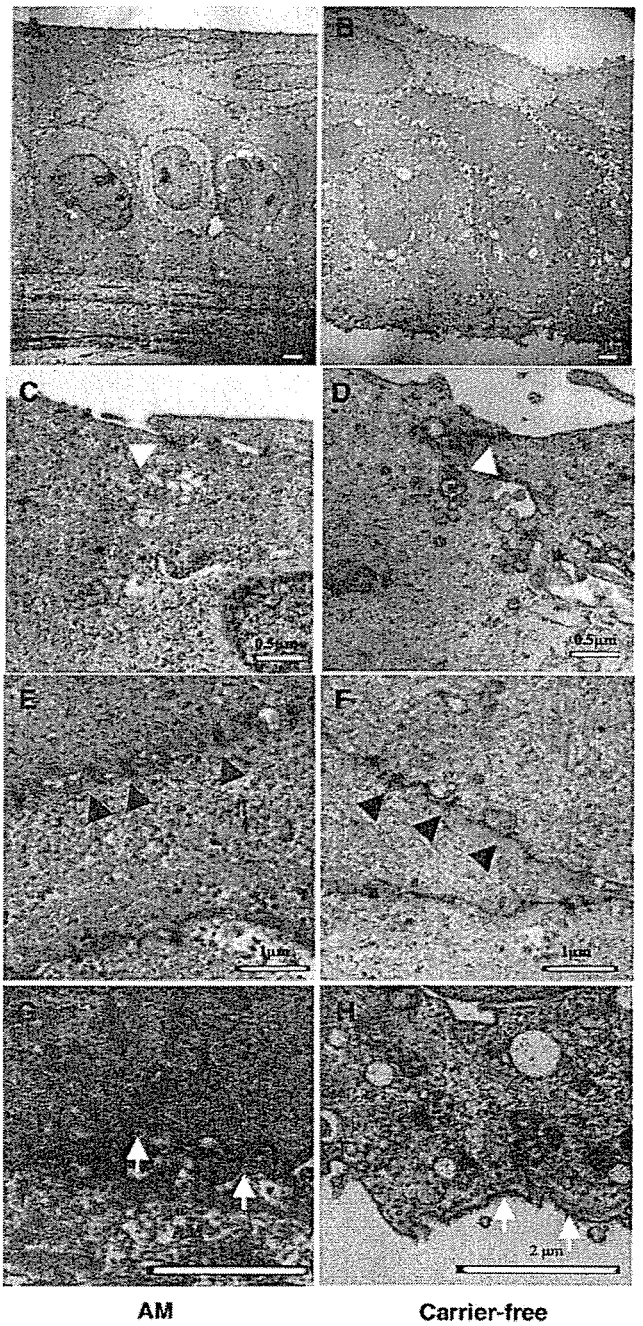

FIGURE 4. Transmission electron micrographs of AM and carrier-free sheets. Both AM (**A**, **C**, **E**, **G**) and carrier-free (**B**, **D**, **F**, **H**) sheets formed five to six layers of well-stratified epithelial cells, with columnar basal epithelial cells. High-magnification views show tight junction formation in apical cells (**C**, **D**, *white arrowheads*), and desmosome formation in the intermediate layers (**E**, **F**, *black arrowheads*). Basal cells formed an intact basement membrane in the AM sheets (**G**, *arrows*), whereas carrier-free sheets had residual material attached to the basal cell membrane (**H**, *white arrows*).

Western Blot Analysis

Epithelial sheets were dissociated with lysis buffer (50 mM Tris-HCl [pH 7.4], 150 mM NaCl, 1% Nonidet P-40; Calbiochem, Darmstadt, Germany) and homogenized. Each epithelial cell sheet was incubated for 40 minutes at 4°C, and then centrifuged at 15,000 rpm for 30 minutes at 4°C. Protein concentration of the supernatant was deter-